1521-0103/386/2/143–155$35.00
THE JOURNAL OF PHARMACOLOGY AND EXPERIMENTAL THERAPEUTICS
dx.doi.org/10.1124/jpet.122.001511
J Pharmacol Exp Ther 386:143–155, August 2023

The Journal of PHARMACOLOGY And Experimental Therapeutics

Special Section on Clinical Pharmacology

Sutimlimab Pharmacokinetics and Pharmacodynamics in Patients with Cold Agglutinin Disease[S]

Thomas Frank, Andreas Kovar, Ashley Strougo,[1] Chandravathi Vage, Nathan Teuscher, and Nancy Wong

Translational Medicine, Pharmacokinetics, Dynamics and Metabolism, Sanofi, Frankfurt, Germany (T.F., A.K., A.S.); Sanofi, Cambridge, Massachusetts (C.V., N.W.); and Certara, Princeton, New Jersey (N.T.)

Received November 16, 2022; accepted April 28, 2023

ABSTRACT

Sutimlimab, a humanized monoclonal antibody targeting the classic complement pathway, is approved in the United States, Japan, and the European Union for the treatment of hemolytic anemia in adults with cold agglutinin disease. The objectives of this study were to support dose selection for phase 3 studies, assess dose recommendations, and establish the relationship between sutimlimab exposure and clinical outcome [hemoglobin (Hb) levels]. Clinically meaningful biomarkers were graphically analyzed and the exposure-response relationship was proposed. The pharmacokinetic (PK) characteristics of sutimlimab were best described by a two-compartment model with parallel linear and nonlinear clearance terms. Body weight was a significant covariate for the volume of distribution in the central compartment (V_c) and total body clearance of sutimlimab. Ethnicity (Japanese, non-Japanese) was a covariate on V_c and maximal nonlinear clearance. There were no PK differences between healthy participants and patients. After graphical exposure-response analysis for biomarkers, a pharmacokinetic-pharmacodynamic model was developed by integrating an indirect response/turnover model for Hb with a maximum effect (E_{max}) model, relating the Hb-elevating effect of sutimlimab to plasma exposure. Renal function and occurrence of blood transfusion were identified as covariates on Hb change from baseline. Simulations showed that E_{max} was attained with the approved dosing (6.5 g in patients <75 kg and 7.5 g in patients ≥75 kg), independent of covariate characteristics, and provided adequate sutimlimab exposure to maximize effects on Hb, bilirubin, and total complement component C4 levels. A change in Hb from baseline at steady state of 2.2 g/dl was projected, consistent with phase 3 study observations.

SIGNIFICANCE STATEMENT

The final validated population pharmacokinetic (PK) and pharmacokinetic/pharmacodynamic (PK/PD) models confirm that the approved dosing regimen for sutimlimab (6.5 g in patients <75 kg and 7.5 g in patients ≥75 kg) is sufficient, without the need for further dose adjustments in populations of patients with cold agglutinin disease.

Introduction

Sutimlimab is a first-in-class, humanized immunoglobulin G 4 monoclonal antibody that targets the classic complement pathway (CP) by selectively inhibiting the complement component 1, s subcomponent (Bartko et al., 2018; Jäger et al., 2019; Röth et al., 2021). Sutimlimab has been approved by the US Food and Drug Administration (FDA), the European Medicines Agency, and in Japan for the treatment of hemolysis in adult patients with cold agglutinin disease (CAD) (https://www.accessdata.fda.gov/drugsatfda_docs/label/2022/761164s000lbl.

This study was funded by Sanofi.
The authors have declared a conflict of interest. T.F. is an employee of a Sanofi company and holds company stock shares. A.K. is an employee of a Sanofi company and holds company stock shares. A.S. is an employee of a Sanofi company. C.V. is an employee of a Sanofi company. N.W. is an employee of a Sanofi company and holds company stock shares. N.T. works as a consultant for Sanofi.
[1]Current affiliation: Oncology Development, Sanofi, Amsterdam, Netherlands.
dx.doi.org/10.1124/jpet.122.001511.
[S] This article has supplemental material available at jpet.aspetjournals.org.

ABBREVIATIONS: AAFE, absolute average fold error; ADA, antidrug antibody; AUC_{ss}, area under the curve at steady state; C4, complement component 4; CAD, cold agglutinin disease; CI, confidence interval; CL, clearance; $C_{max,ss}$, maximum concentration at steady state; $C_{min,ss}$, minimum concentration at steady state; CLCR, creatinine clearance; CP, complement pathway; E_{base}, Hb baseline; eGFR, estimated glomerular filtration rate; E_{max}, maximum effect; GI, gastrointestinal; Hb, hemoglobin; IC_{90}, concentration of drug required for 90% inhibition; IIV, interindividual variability; IPRED, individual predicted data based on individual empirical Bayes parameter estimates; k_{out}, first-order dissipation rate constant; MAP, maximum a posteriori; MPE, mean prediction error; NONMEM, nonlinear mixed-effects modeling; NPDE, normalized prediction distribution errors; pcVPC, prediction-corrected visual predictive check; PD, pharmacodynamic(s); PK, pharmacokinetic(s); popPK, population pharmacokinetics; PRED, predicted data based on population parameter estimates; RMSE, root mean squared error; V_c, volume of distribution of the central compartment; VPC, visual predictive check.

pdf; https://www.ema.europa.eu/en/documents/product-information/enjaymo-epar-product-information_en.pdf).

CAD is a rare type of autoimmune hemolytic anemia, mediated by persistent complement activation via the classic CP leading to hemolysis (Berentsen, 2016; Röth et al., 2021), and an increased risk of thromboembolism (Chapin et al., 2016; Mullins et al., 2017; Bylsma et al., 2019; Broome et al., 2020; Jäger et al., 2020; Kamesaki et al., 2020; Delvasto-Nunez et al., 2021). Vascular symptoms such as acrocyanosis and Raynaud's phenomenon are not present in all patients with CAD (Berentsen et al., 2015, 2020). Other symptoms of CAD including fatigue, dyspnea, weakness, dark urine, jaundice, and weight loss are nonspecific, which can complicate initial disease recognition and diagnosis (Berentsen, 2016; Röth et al., 2021).

The pharmacokinetics (PK) and pharmacodynamics (PD) of sutimlimab were first investigated in healthy participants in a phase 1 study (Bartko et al., 2018). In this study, the mean sutimlimab exposure increased in a greater than dose-proportional manner in the dose range of 3–30 mg/kg and in an approximately dose-proportional manner in the higher dose range of 60–100 mg/kg (Bartko et al., 2018). Complete inhibition of CP activity was achieved in all participants who received a sutimlimab dose of 3 mg/kg or higher. The duration of CP inhibition was dose related (Bartko et al., 2018).

The phase 3 CARDINAL (BIVV009-03; NCT03347396) and CADENZA (BIVV009-04; NCT03347422) trials examined the effect of sutimlimab in patients with CAD with or without a recent history of transfusion, respectively (Röth et al., 2021, 2022). In both trials, sutimlimab rapidly halted hemolysis and increased hemoglobin (Hb) levels. The activity of the classic CP was almost completely inhibited within 1 week after the initiation of sutimlimab treatment, with concomitant normalization of complement component 4 (C4) levels (Röth et al., 2021). The PK characteristics of sutimlimab in patients with CAD have not been published. The recommended dosage of sutimlimab for pivotal phase 3 studies was 6.5 g for patients weighing between 39 kg and less than 75 kg, and 7.5 g for patients weighing greater than or equal to 75 kg. This was administered by intravenous infusion over 1 to 2 hours once weekly for the first two doses, followed by every 14 days thereafter (https://www.accessdata.fda.gov/drugsatfda_docs/label/2022/761164s000lbl.pdf; https://www.ema.europa.eu/en/documents/product-information/enjaymo-epar-product-information_en.pdf).

The objectives of this study were to support dose selection for phase 3 studies, to assess the effectiveness of the approved dose recommendation, to determine whether any further dose adjustments may be required, and to establish the relationship of sutimlimab exposure and clinical outcome (i.e., Hb levels). Population PK (popPK) and PK/PD models were developed to account for intersubject variability and the effects of covariates on PK of sutimlimab and Hb, respectively. In addition, clinically meaningful biomarkers Hb, bilirubin and C4 values were graphically evaluated and the exposure-response relationship was proposed. Bilirubin is a recognized marker of extravascular hemolysis in CAD patients. C4 is the first soluble cleavable substrate of the C1 complex, the target of sutimlimab.

Materials and Methods

Study Design and Patient Population

Data from the studies listed in Table 1 were included in the analyses. Detailed information on study design, dosing, and inclusion/exclusion criteria have been published previously (Mühlbacher et al., 2017; Bartko et al., 2018; Jäger et al., 2019; Röth et al., 2021, 2022). These studies were conducted according to the International Conference on Harmonization Good Clinical Practice Guideline and the Declaration of Helsinki and were approved by local independent ethics committees or review boards. Participants provided written informed consent.

Model Development

The popPK model was developed with data from studies BIVV001-01, BIVV009-02, BIVV009-03, and BIVV009-05 and was further validated with a larger dataset as described in model validation. PK/PD model development included data from studies BIVV009-01 parts C and E, BIVV009-03 parts A and B, BIVV009-04 part A, and was evaluated later using final data from part B of studies BIVV009-03 and BIVV009-04.

1. First structural and random models were identified including interindividual variability (IIV) assessment.
2. After selection of the optimal structural PK or PK/PD model, trends in empirical Bayes estimates versus categorical and continuous covariates were graphically tested first and identified for covariate model development and covariate analysis. A list of all covariates can be found in Supplemental Methods (Population PK-PD Model Development; Population PK Model Development). Covariates were only considered on model parameters with identifiable IIV. The impact of identified covariates was then systematically evaluated using the forward-addition ($P = 0.01$) and backward-deletion ($P = 0.001$) methods. Evaluation of the quality of both the PK and PK/PD models was based on likelihood of the data (objective function value) goodness-of-fit plots, η-shrinkage, quality criteria, visual predictive check (VPC), and simulations.
3. The selected covariate model was then qualified by prediction-corrected visual predictive checks (pcVPCs) and bootstrap analysis.

PopPK Model

The analysis population consisted of all evaluable participants, defined as those who had at least one postdose sutimlimab concentration sample greater than the lower limit of quantitation (5 ng/ml) and an associated dosing and blood sampling record for the postdose sample.

Structural and random models were identified first, followed by covariate model development. Relationship of the following covariates was evaluated on volume parameters: age, body weight, sex, race, Japanese ethnicity, renal function by creatinine clearance (CLCR), and estimated glomerular filtration rate (eGFR), hepatic function [serum aspartate transaminase (AST), albumin], and disease status. Relationship of the following covariates was evaluated on clearance parameters: age, body weight, sex, race, Japanese ethnicity, CLCR, eGFR, measures of hepatic function, and disease status (Supplemental Table 1). The impact of antidrug antibody (ADA), diluted infusion, and occurrence of blood transfusion was graphically evaluated after availability of the complete dataset, as part of model evaluation. The final popPK model was then used to simulate expected profiles of potential populations of interest and further used to estimate exposure parameters of sutimlimab [minimum concentration at steady state ($C_{min,ss}$), maximum concentration at steady state ($C_{max,ss}$), area under the curve at steady state (AUC_{ss})] in patients with CAD. Further information on the PK model development methodology and evaluation is provided in Supplemental Methods (Model Evaluation; Population PK Model Development; Supplemental Tables 2 and 3).

Exposure-Response Analysis

Graphical Exploration of Biomarkers. Observed biomarker (Hb, bilirubin, and C4) and change in biomarker from baseline in patients with CAD were selected for the analysis. This comprised the creation of individual and dose group plots for observed and change (median, maximum, and 95th percentile) from baseline levels. An exploratory characterization of the exposure-response relationship was also attempted. A maximum effect (E_{max}) model was fitted to the change in Hb or C4 from baseline, and a maximum inhibitory effect (I_{max}) model was fitted to the change in bilirubin from baseline versus time-matched observed $C_{min,ss}$.

PopPK/PD Model. A dynamic popPK/PD structural model for Hb was developed by linking the complete time profile of sutimlimab concentrations to the time profiles of Hb. The PK component consisted of the final popPK model; the PD component was based on an indirect response/turnover model for Hb dynamics over time, including a zero-order rate constant (k_{in}) for Hb production and a first-order rate constant (k_{out}) for elimination of Hb, which is inhibited by sutimlimab concentration in the central compartment (Supplemental Fig. 1). Structural and random models were initially identified, followed by covariate model development (Supplemental Methods: Population PK-PD Model Development). The covariates investigated were age, body weight, sex, race, ethnicity (Japanese/non-Japanese), blood transfusion, eGFR, CLCR, and measures of hepatic function (i.e., albumin, AST, serum alanine transaminase, and bilirubin) (Supplemental Table 4). The impact of ADA and dilution of infusion was graphically evaluated. Further information on the popPK/PD model is provided in Supplemental Methods (Model Evaluation; Population PK-PD Model Development).

Model Validation

Maximum a posteriori (MAP) probability Bayesian approach was applied to larger datasets to validate previously developed covariate models. The popPK and PK/PD full covariate models obtained in model development were applied to a dataset, including data from prior analysis used for model development and additional data from completed studies (mainly BIVV009-03 and BIVV009-04), with prior population parameter estimates for the assessment of individual parameters and concentration predictions.

As the larger datasets were submitted to a MAP Bayesian analysis, potential new covariates were not included in the model and tested for statistical significance again. Instead, individual random subject effect estimates (η) were plotted versus covariates already investigated in previous analysis, such as ADA status, occurrence of blood transfusion, and administration of diluted/undiluted infusion. The approach is justified because the η-shrinkage was within an acceptable range.

Model evaluation was performed by standard goodness-of-fit plots, investigation of covariates, prediction-corrected VPC, and quality criteria such as mean prediction error (MPE), root mean squared error (RMSE), and absolute average fold error (AAFE). Further information on the model evaluation is provided in Supplemental Methods (Model Evaluation). Trends in empirical Bayes estimates versus categorical and continuous covariates were graphically tested (box and scatter plots). Absence of covariate effect was concluded if there was no major trend.

Dose Selection

Concentration versus CP activity inhibition relationship was evaluated using data from BIVV001 Parts A–C and BIVV009-02 studies in healthy participants and patients. Individual serum concentrations of sutimlimab and CP activity were time-matched, and the PK/PD relationship was modeled using an inhibitory E_{max} model as described below:

$$E = E_0 - \frac{I_{max} * C^H}{C^H + IC_{50}{}^H} \quad (1)$$

where E_0 is the baseline, I_{max} is the maximum inhibition, C is the concentration of sutimlimab, IC_{50} is the concentration associated to 50% of the maximum effect, and H is the Hill factor (also referred as gamma, a parameter used to describe sigmoidicity). It was assumed that a similar relationship existed in healthy participants and patients. The 90% inhibition (IC_{90}) was identified graphically and was estimated from IC_{50} of PK/PD relationship. The IC_{90} was used as threshold concentration for dose selection.

The popPK model was used to simulate the dose required in 97 participants (66 healthy subjects and 31 patients from two phase 1 studies) to maintain concentrations above threshold concentration when administered once weekly for 1 week and biweekly thereafter. The weekly regimen for the first few doses was proposed to achieve rapid increase in concentrations due to the expected steep nature of the PD response and rapidly saturating processes that cause nonlinearities in PK. The threshold concentration in participants was justified based on most of the observed concentrations displaying nonlinearities below these levels, exacerbating risk for breakthroughs occurring rapidly given likely dosing deviations. As such, maintaining levels above threshold concentration would be expected to provide an additional concentration buffer for dosing deviations or unexpected variability in PK. Percentage of participants with $C_{min,ss}$ above threshold concentration was estimated. The sutimlimab dose for pivotal phase 3 studies was selected based on maximum percentage of participants with estimated $C_{min,ss}$ above the threshold concentration.

Simulations were performed representing populations (including the various sources of IIV). For the stochastic simulations, dose and covariates were sampled from the observed data considering potential correlations among them. In the deterministic simulations, covariates were kept at median values except for the covariate under evaluation. Covariates were evaluated using the minimum and maximum values from the observed data. Each participant in the dataset was simulated 100 times. In total, 17,600 virtual participants for PK and 7200 for Hb were simulated. The simulations were statistically summarized using median (defined by the 50th percentile of the simulated values) and 90% prediction interval (defined by the 5th and 95th percentiles of the simulated values).

Exposure-Safety Analysis

Individual empirical Bayesian PK parameter estimates obtained from the popPK analysis were used to simulate PK profiles and to derive individual sutimlimab PK exposure metrics contingent on each participant's actual dosing records (Supplemental Methods: Exposure Parameters). Systemic sutimlimab-exposure metrics were obtained, including AUC_{ss} and $C_{max,ss}$. Sutimlimab PK exposure metrics were categorized by quartiles, and the rates of selected safety events (infections and infestations, gastrointestinal disorders, vascular disorders, skin and subcutaneous tissue disorders, general disorders and administration site conditions, musculoskeletal and connective tissue disorders, nervous system disorders, injury, poisoning and procedural complications, respiratory disorders) were compared across the quartile categories. These analyses were performed for all participants who took part in BIVV009-03 and BIVV009-04 studies.

Dose-Safety Analysis

Sutimlimab doses per kg body weight were categorized by quartiles, and the rates of safety events described above were compared across the quartile categories. The same analysis was repeated with body weight quartiles.

Software and Computational Approach

Nonlinear mixed-effects modeling software (NONMEM) (version 7.4; ICON, Hanover, MD) was used for popPK and PK/PD modeling of Hb data. The first-order conditional estimation method of NONMEM with IIV and residual variability interaction (FOCE INTER) was used for model development. For MAP Bayesian analysis, the estimation step was omitted using the NONMEM option MAXEVAL = 0 to

TABLE 1
Clinical study design, dosing, and sampling for studies involved in the analyses

Study	Description	Participants	Dosing	PK Sampling[a]	PD Sampling[b]
BIVV009-01 NCT02502903	Phase 1 safety, tolerability, and activity of sutimlimab in healthy participants and patients with complement-mediated disorders	Part A: 36 healthy participants (6 per cohort) Part B: 12 healthy participants (6 per cohort) Part C: 34 patients with various complement-mediated disorders Part E: four patients with CAD continuing from part C	Part A: single dose of 0.3 mg/kg ascending through 100 mg/kg Part B: weekly dosing of 30 or 60 mg/kg for 4 weeks Part C: single dose (10 mg/kg) and subsequent weekly dosing at 60 mg/kg for 4 weeks Part E: day 0, week 1, and every 2 weeks thereafter until the last visit; 5.5 g sutimlimab followed by fixed dose of 6.5 g (patients weighing <75 kg) or 7.5 g (patients weighing ≥75 kg)	Parts A and B: predose; 0.5, 1, 4, 8, 24, 48, 72, 96, and 168 hours postdose; EOS/ET Part C, day 0: predose and 1, 4, 8, 24, and 48 hours postdose; days 4, 11, and 18: predose and 1 and 4 hours postdose; day 25: predose and 1, 4, 48, 96, and 168 hours postdose; days 39, 46, and 53 Part E, days 0, 7, 21: predose; predose every 14 days at each further treatment visit after day 21; EOS/ET	Parts A and B were not used in the analysis. Part C, day 0: predose and 1, 4, 8, 24, and 48 hours postdose; days 4, 11, and 18: predose and 1 and 4 hours postdose; day 25: predose and 1, 4, 48, 96, and 168 hours postdose; days 39, 46, and 53 Part E, days 0, 7, 14–21: predose, EOS/ET and safety follow up (9 weeks after last dose)
BIVV009-02	Phase 1 safety, tolerability, PK, and PD of multiple-dose sutimlimab in healthy participants	18 male and female healthy participants	75 mg/kg on days 1, 8, 22, and 36	Day 1: predose and 0.5, 1, 4, 8, 24, 48, 72, 96, and 168 hours postdose Days 8 and 22: predose and 4 hours postdose Day 36: predose; 0.5, 1, 4, 8, 24, 48, 72, 96, 168 hours postdose; and EOS/ET	
CARDINAL (BIVV009-03) NCT03347396	Phase 3 open-label, single-arm, multicenter study in patients with primary CAD who have a recent history of blood transfusion	24 patients with primary CAD who have a recent history of transfusion	Patients <75 kg: fixed dose of 6.5 g (N = 17) Patients ≥75 kg: fixed dose of 7.5 g (N = 7) Part A: dose administered on day 0, day 7, and every 14 days thereafter through week 25 Part B: immediately followed after part A every 14 days for 2 years	Part A: predose and 1 hour (±15 min) postdose on days 0, 7, 21, 35, 49, 63, 77, 91, 105, 119, 133, 147, 161, and 175; EOT (day 182)/ET Part B: samples were collected at 3-month intervals during the first year of treatment in part B and then at 6-month intervals for the remainder of the time on study. Samples were collected if a patient experienced a hematologic breakthrough event or withdrew from the study.	Part A: predose and 1 hour (±15 min) postdose (i.e., 1 hour after completion of study drug infusion) on days 0, 7, 21, 35, 49, 63, 77, 91, 105, 119, 133, 147, 161, and 175; EOT (day 182)/ET Part B: samples were collected at 3-month intervals during the first year of treatment in part B and then at 6-month intervals for the remainder of the time on study. Samples were collected if a patient experienced a hematologic breakthrough event or withdrew from the study.
CADENZA (BIVV009-04) NCT03347422	Phase 3 randomized, double-blind, placebo-controlled multicenter study	42 patients with primary CAD without a recent history of transfusion	Part A: 20 patients received placebo; patients <75 kg: fixed dose of 6.5 g (N = 35);	Part A: predose and 1 hour (±15 min) postdose on days 0, 7, 21, 35, 49, 63, 77, 91,	Part A: predose and 1 hour (±15 min) postdose (i.e., 1 hour after completion of

TABLE 1 *continued*

Study	Description	Participants	Dosing	PK Sampling[a]	PD Sampling[b]
	in patients with primary CAD without a recent history of blood transfusion		patients ≥75 kg: fixed dose of 7.5 g (N = 8) Part A: dose administered on day 0, day 7, and every 14 days thereafter through week 25 Part B: crossover loading dose at week 26; biweekly dosing starting at week 27 and continuing for 1 year after LPO under part A	105, 119, 133, 147, 161, and 175; EOT (day 182)/ET Part B: (±15 min) postdose on days 189, 217, and 245, then routinely at 3-month intervals starting at day 273 through the remainder of the study. Samples were also collected if a patient experienced a hematologic breakthrough event or withdrew from the study.	study drug infusion) on days 0, 7, 21, 35, 49, 63, 77, 91, 105, 119, 133, 147, 161, and 175; EOT (day 182)/ET Part B: predose and 1 hour (±15 min) postdose on days 189, 217, and 245, then routinely at 3-month intervals starting at day 273 through the remainder of the study. Samples were also collected if a patient experienced a hematologic breakthrough event or withdrew from the study.
BIVV009-05	Phase 1 safety, tolerability, PK, and PD of sutimlimab in healthy Japanese participants	Part A: 18 healthy Japanese participants (6 per cohort) Part B: 12 healthy Japanese participants	Part A: single dose of 30 mg/kg, 60 mg/kg, and 100 mg/kg Part B: fixed dose of 6.5 g on days 1, 8, and 22 in healthy participants <75 kg (N = 9) and fixed dose of 7.5 g on days 1, 8, and 22 in healthy participants ≥75 kg (N = 3)	Part A: predose, 0.5, 1, 4, 8, 24, 48, 72, and 96 hours postdose and on days 8 and 15 Part B: day 1 and 22: Predose and 0.5, 1, 8, 24, 48, 72, and 96 hours postdose; day 8: predose and 4 hours postdose; days 29, 36, 50, and 85	

EOS, end of study; EOT, end of treatment; ET, early termination; LPO, last patient out.
[a]The popPK model was developed with data from healthy participants and patients from BIVV00-01, BIVV009-03, BIVV009-02, and BIVV009-05. This model was evaluated with additional final PK data from the phase 3 studies BIVV009-03 and BIVV009-04.
[b]The exposure-response (PK/PD) model was developed with data from patients with CAD from BIVV009-01 part C and BIVV009-03 part A. This model was evaluated with additional final PD data from BIVV009-01 part E, BIVV009-03 part B, and BIVV009-04 parts A and B.

compute the individual estimates based on the population estimates of θ, ω, and σ obtained in the full covariate model.

SAS (version 9.4) or R (version 3.6) was used for data preparation, model diagnostics, statistical summaries, and simulations. Graphical exposure-response analysis was conducted using rstanemax package (version 0.1.3) in R. Information on handling of missing or erroneous data is provided in Supplemental Methods (Handling of Missing or Erroneous Data).

Results

Data Accounting and Baseline Demographics

The final PK model parameters were estimated during model development using 2470 PK observations from 154 participants. The percentage of postdose PK observations below the quantification limit (BLQ) was 7%. The final PK analysis dataset for model evaluation using the Bayesian approach included 4140 evaluable observations from 196 participants (healthy subjects and patients). The percentage of postdose BLQ observations was 6%. The final PK/PD model parameters were estimated during model development using 2368 Hb concentrations from 72 patients with CAD. The final PK/PD analysis dataset for model evaluation using the Bayesian approach included 4269 Hb observations from 72 patients with CAD (all participants from studies BIVV009-03 and BIVV009-04 and six from study BIVV009-01 part C with four of them progressing into part E). The baselines characteristics for both datasets are shown in Table 2. In total, eight participants in studies BIVV009-03 and BIVV009-04 were ADA positive, and 22 participants in studies BIVV009-03 and BIVV009-04 received blood transfusion.

PopPK Model

Several potential structural models were investigated [one or two compartments, mixed-linear and nonlinear (Michaelis-Menten) elimination]. A two-compartment model with Michaelis-Menten elimination best described the sutimlimab data. IIV terms were included on clearance (CL), volume of distribution of the central compartment (V_c), volume of distribution of the peripheral compartment (V_p), and maximum nonlinear clearance (V_{max}). The residual error model includes additive and proportional error terms for the BIVV009-03 study and separate additive and proportional error terms for non–BIVV009-03 studies. Parameter estimates from the final popPK model are summarized in Table 3.

TABLE 2
Baseline characteristics by studyThe final PK analysis dataset included 196 participants (healthy participants and patients from all five studies). The number of participants from each study/cohort can be found in Table 1.

	Study					
Characteristic	BIVV009-01 $N = 82$	BIVV009-01 Part C[a] (Subset of $n = 6$ patients with CAD)	BIVV009-02 $N = 18$	BIVV009-03 $N = 24$	BIVV009-04 $N = 42$	BIVV009-05 $N = 30$
Age, mean (S.D.)	45.5 (19.7)	69.7 (7.66)	33.3 (8.42)	71.3 (8.18)	66.7 (10.5)	41.8 (9.01)
Sex (female, %)	50.0	100	5.60	62.5	78.6	16.7
Race (%)						
White	95.1	100	50.0	12.5	9.5	0
Black/African American	2.40	0	44.4	0	0	0
Asian/Japanese	1.20	0	5.60	12.5	16.7	100
Other/missing	1.20	0	0	75.0	73.8	0
Disease status (%)						
Healthy	58.5	0	100	0	0	100
CAD	12.2	100	0	100	100	0
Other	29.3	0	0	0	0	0
Negative ADA status (%)	91.5	83.3	77.8	91.7	85.7	90.0
Received ≥1 blood transfusion during the study (%)	0	100	0	41.7	28.6	0
Weight (kg), mean (S.D.)	73.2 (13.1)	71.6 (7.72)	80.7 (15.9)	67.8 (15.8)	65.9 (12.1)	68.6 (13.3)
CLCR (ml/min), mean (S.D.)	99.0 (37.4)	69.5 (14.8)	124 (24.3)	71.5 (33.2)	81.4 (24.7)	122 (22.2)
eGFR (ml/min/1.73 m^2), mean (S.D.)	83.2 (29.9)	68.5 (23.1)	98.9 (17.8)	77.4 (27.5)	85.7 (20.1)	112 (18.0)
Albumin (g/l), mean (S.D.)	0	0	45.9 (4.71)	40.9 (3.05)	41.9 (2.35)	47.3 (2.39)
Bilirubin (mg/dl), mean (S.D.)	0.91 (1.39)	2.76 (1.28)	0.79 (0.27)	2.98 (1.37)	2.26 (1.19)	0.800 (0.260)
Hb (g/dl), mean (S.D.)	ND	7.68 (0.54)	ND	8.59 (1.61)	9.24 (1.03)	ND
C4 (g/l), mean (S.D.)	ND	0.110 (0.050)	ND	0.040 (0.070)	0.060 (0.060)	ND

ND, not determined.
[a]The final PD dataset included 72 patients with CAD (6 participants from study BIVV009-01 parts C and E and all participants from BIVV009-03 and BIVV009-04).

Body weight and Japanese ethnicity were found to be statistically significant covariates for CL and V_c, and Japanese ethnicity was found to be a significant covariate for V_c and V_{max}. In addition, age had a significant effect on V_c (Table 3). After including age, body weight, and Japanese participant covariates, the following covariates did not have an additional effect on the PK of sutimlimab: sex, race, albumin, hepatic function, renal function, and disease status. The effect of ADA was graphically evaluated.

Evaluation of the PK model using all data showed good agreement between predictions and observations in the goodness-of-fit plots in general (Supplemental Fig. 2). Quality criteria and pcVPC showed an acceptable performance of the model to describe the data (Supplemental Figs. 3 and 4; Supplemental Table 5). Simulation-based diagnostics using mean normalized prediction distribution errors (NPDE) do support the results of goodness-of-fit plots. Overall, the mean NPDE was 0.0255 ($P = 0.21$) with a variance of 0.866 ($P < 0.001$), indicating no bias and an ability of the model to reasonably capture the underlying variability (Supplemental Fig. 5). The MPE of the population predictions was small, with −1.18% of the observations with zero of the absolute MPE

TABLE 3
Parameter estimates of the full covariate popPK model

Population Parameters (Unit)	Estimate (Mean)	%RSE[a]	IIV (Mean)[a]	%RSE[a]	η-Shrinkage[b] (%)
Clearance (CL, ml/h)	5.69	6.29	33.7	18.8	34.8
Effect of body weight on CL[c]	1.71	10.7	ND	ND	ND
Intercompartmental clearance (Q, ml/h)	19.8	7.63	ND	ND	ND
Central volume of distribution (V_c, l)	3.83	2.09	19.3	6.15	5.80
Effect of body weight on V_c[c]	0.536	16.4	ND	ND	ND
Japanese ethnicity effect on V_c	−0.285	9.89	ND	ND	ND
Age effect on V_c[d]	0.182	21.8	ND	ND	ND
Peripheral volume of distribution (V_p, l)	1.98	6.96	54.7	17.1	22.8
Maximal nonlinear clearance (V_{max}, mg/h)	9.85	3.36	19.7	13.7	24.8
Japanese ethnicity effect on V_{max}	−0.300	19.7	ND	ND	ND
BIVV009 concentration required for half-maximal nonlinear clearance (K_m, μg/ml)	8.61	24.6	ND	ND	ND
Residual variability:					
BIVV009-03 study proportional residual error	0.267	17.9	NA	NA	NA
BIVV009-03 study additive residual error S.D. (μg/ml)	110	25.5	NA	NA	NA
Non–BIVV009-03 studies proportional residual error	0.141	9.02	NA	NA	NA
Non–BIVV009-03 studies additive residual error S.D. (μg/ml)	5.93	19.6	NA	NA	NA

%CV, percent coefficient of variation; NA, not applicable; ND, not determined; RSE, relative standard error.
[a]RSEs of parameter estimates are calculated as 100 × (S.E./typical value); estimates (mean) of IIV are presented as %CV; RSEs of IIV magnitude are presented on %CV scale and are approximated as 100 × (S.E./variance estimate)/2.
[b]Shrinkage (%) is calculated as 100 × (1 − S.D. of post hocs/estimated variance).
[c]Effect of body weight is relative to the median body weight of 71.85 kg.
[d]Effect of age is relative to the median age of 43.5 years.

included in the 95% confidence interval (CI). The relative MPE of individual predicted data based on individual empirical Bayes parameter estimates (IPRED) indicated a minor underprediction of −1.58% of the observations. The precision of the model was reasonable, with an RMSE of 45.2% and 27.1% for predicted data based on population parameter estimates (PRED) and IPRED, respectively. AAFE was 1.37 and 1.17 for PRED and IPRED, respectively, and thus near the optimal value of 1 (Supplemental Table 5).

Box and scatter plots of the individual post hoc estimates of random effects versus body weight, age, ethnicity, race, sex, ADA status, disease status, occurrence of blood transfusion, infusion dilution, and measures of renal and hepatic function did not reveal marked correlation that would require correction of the covariate model (data not shown).

The mean changes of post hoc $C_{min,ss}$ $C_{max,ss}$, and AUC_{ss} at steady state ranged from 0.7 to 0.8 in patients weighing ≥75 kg, from 1.2 to 1.4 in Japanese patients, and from 0.8 to 1.0 in elderly patients compared with the reference populations. The calculated 95% CIs overlap 1 in many instances (Fig. 1).

Graphical Exploration of Biomarkers

Hemoglobin and C4 levels increased and bilirubin decreased after administration of sutimlimab in patients with CAD. After placebo treatment, there were no visible changes over time for Hb, bilirubin, and C4 (Fig. 2). The median observed changes from baseline at steady state following the approved regimen were 2.6 g/dl for Hb, 0.23 g/l for C4, and −1.7 mg/dl for bilirubin; and the median biomarker levels at steady state were 11.8 g/dl for Hb, 0.28 g/l for C4, and 0.801 mg/dl for bilirubin after 6.5 or 7.5 g sutimlimab.

$C_{min,ss}$ and change in biomarkers were time matched for characterization of exploratory PK/PD relationship. The estimated E_{max} (Hb and C4) or I_{max} (bilirubin) captured maximum observed effect on biomarker. The estimated $C_{min,ss}$ for half-maximum effect on Hb and bilirubin (EC_{min} for Hb, IC_{min} for bilirubin) were 50.7 to 298 μg/ml with all observed $C_{min,ss}$ (Supplemental Fig. 6).

PK/PD Model

The time course of Hb was modeled using a turnover model, including k_{in} for Hb production and k_{out} for elimination of Hb, which is inhibited by sutimlimab concentration in central compartment. IIV was identified for Hb baseline (E_{base}) and E_{max}. Significant covariates were CLCR on E_{base} and blood transfusion status (binary covariate) on E_{max}. After including CLCR and blood transfusion as covariates, the following covariates did not reveal marked correlation with model parameters: body weight, age, ethnicity, race, sex, ADA status, disease status, infusion dilution, and measures of renal and hepatic function. The parameter estimates for the final PK/PD model are shown in Table 4. All parameters were estimated with reasonable precision and IIV was described with acceptable η-shrinkage.

Goodness-of-fit plots generally showed a good agreement between predicted and observed Hb levels, as they form a relatively close distribution around the identity line. The population predictions at lower Hb levels were slightly underpredicted (Supplemental Fig. 7).

Evaluation of the Hb PK/PD model showed good agreement between predictions and observations in the goodness-of-fit plots (Supplemental Fig. 8). Quality criteria and VPC also showed an acceptable performance of the model to describe the data (Supplemental Figs. 8 and 9; Supplemental Table 6). Simulation-based diagnostics using mean NPDE do support the results of goodness-of-fit plots. Overall, the mean NPDE was 0.00261 ($P = 0.058$) with a variance of 1.21 ($P < 0.001$), indicating no bias and a tendency of the model to overpredict the underlying variability (Supplemental Fig. 10). However, the NPDE versus time and PRED show no trend, indicating an adequate performance of the model to describe the Hb observations. The MPE of the population predictions was small with −1.76% of the observations (zero of absolute MPE not included in 95% CI). The MPE of IPRED was negligible with 0.013% of the observations (zero of absolute MPE included in 95% CI). The precision of the model was good, with an RMSE of 14.4% and 9.2% for PRED and IPRED, respectively. AAFE was 1.12 and 1.07 for PRED and IPRED, respectively, and thus near the optimal value of 1 (Supplemental Table 6).

Box and scatter plots of the individual post hoc estimates of random effects versus body weight, age, ethnicity, race, sex, ADA status, disease status, occurrence of blood transfusion, infusion dilution, and measures of renal and hepatic function did not reveal marked correlation that would require correction of the covariate model (data not shown).

Dose Selection

Near-maximal classic CP activity inhibition was observed for sutimlimab concentrations >20 μg/ml (Fig. 3). A steep concentration-effect relationship was observed for the inhibition of CP activity. Based on the inhibitory E_{max} model, a 50% inhibition of CP activity was predicted at 6.2 μg/ml sutimlimab, and that of an IC_{90} was 15.5 μg/ml. The very low IC_{50} combined with a Hill parameter of 2.4 suggests a very steep concentration-effect relationship and that sutimlimab concentrations above 100 μg/ml would be sufficient to maintain a near-maximal knockdown of CP activity and avoid nonlinear PK. The final popPK model was used to simulate steady-state concentration in patients with CAD. Three dose levels were simulated for comparison: 5.5 g, 75 mg/kg, and the approved regimen of 6.5 g for body weight <75 kg and 7.5 g for body weight ≥75 kg. The approved regimen of 6.5 g for body weight <75 kg and 7.5 g for body weight ≥75 kg (6.5 g/7.5 g) was selected based on the predicted exposure being above 100 μg/ml in the maximum number of patients. The cutoff value of 75 kg was selected to coincide with the median body weight of 631 participants extracted from a US electronic medical record and claims database. This 6.5-g/7.5-g tiered dosing regimen was predicted to maintain target trough concentrations >100 μg/ml throughout the dosing period in approximately 94% of patients with CAD (Supplemental Table 7) to minimize the risk of breakthrough hemolysis while providing sufficient safety margins. The data from BIVV009-03 and BIVV009-04 studies showed only seven patients (7/66 = 10.6%) with trough levels below 100 μg/ml during the treatment period without dose interruption, which was consistent with the predicted values based on the popPK model, 6.2% (90% CI: 2.0%–12.0%).

The final popPK and PK/PD models were used to simulate exposures (Fig. 4) and Hb profiles (Fig. 5) at the approved dosing regimen for adult patients (6.5-g dose in patients who weigh <75 kg and 7.5-g dose in patients who weigh ≥75 kg). Doses were administered on day 0, day 7, and then every 14 days thereafter through week 125.

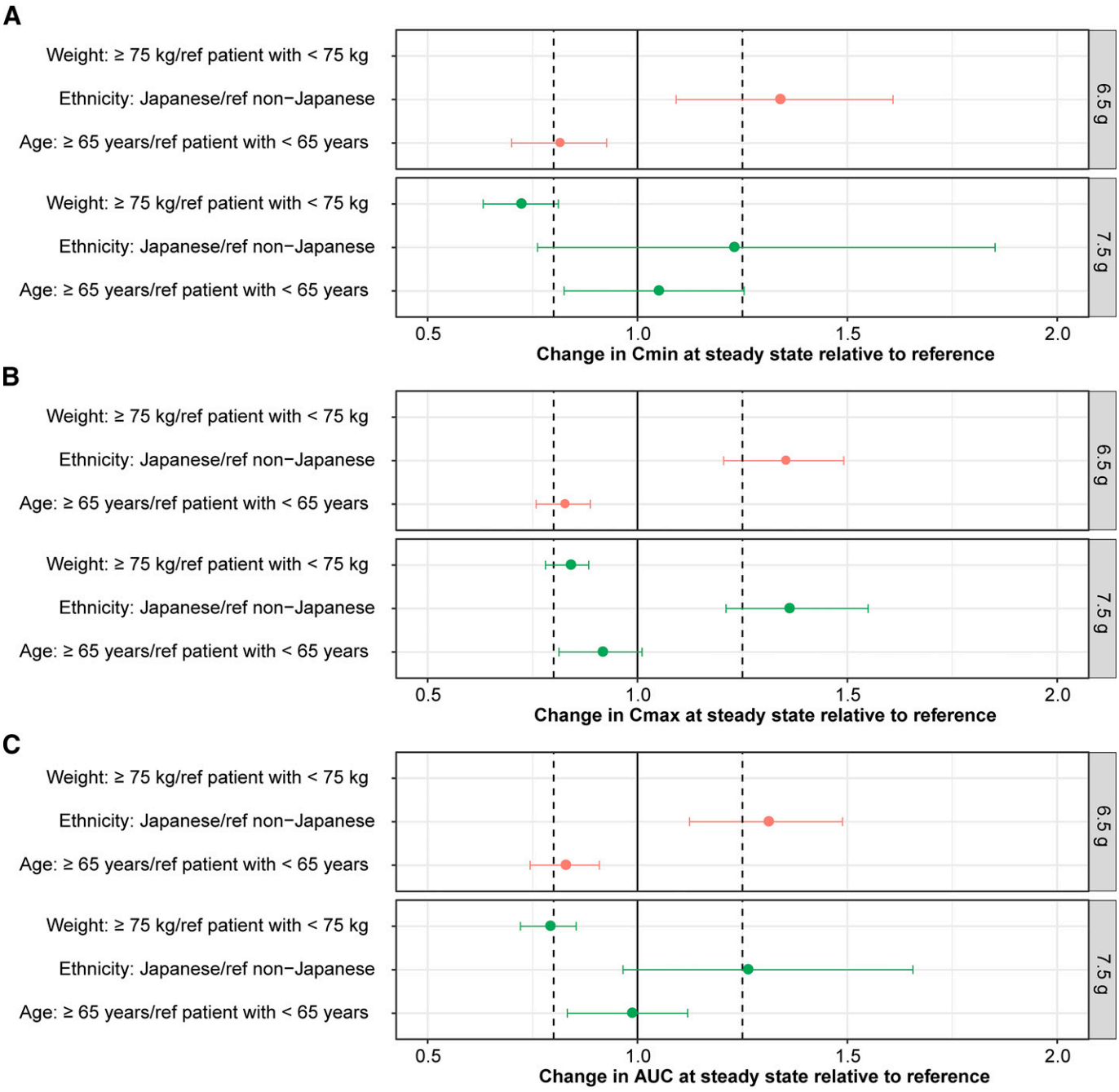

Fig. 1. Change in $C_{min,ss}$ (A), $C_{max,ss}$ (B), and AUC_{ss} (C) at steady state relative to the reference population. Individual post hoc estimates of $C_{min,ss}$, $C_{max,ss}$, and AUC_{ss} at steady state were calculated using the approved sutimlimab dosing regimen (6.5 g in red, 7.5 g in green). The solid circles represent the mean values, with error bars representing the 95% CI.

Stochastic simulations of the evaluation of the impact of dose (6.5 g in patients <75 kg and 7.5 g in patients ≥75 kg) stratified by minimum (39 kg) and maximum (112 kg) body weights showed the Hb change from baseline time profiles to be very similar (Fig. 6).

The impact of statistically significant PK and PD covariates on the typical changes in Hb from baseline at steady state with the approved dosing regimen was shown to be of 1.2-fold change for a patient weighing 39 kg compared with 112 kg, of 1.3-fold change increase for a patient with CLCR value of 174 ml/min compared with a patient with CLCR value of 24 ml/min, and of 1.9-fold change for a patient without occurrence of transfusion compared with a patient with occurrence of transfusion. No impact of ethnicity or age was observed (Supplemental Fig. 11).

Exposure-Safety Analysis

The proportions of patients with selected safety events by serum sutimlimab-exposure quartiles are provided in Supplemental Results (Supplemental Figs. 12 and 13) for the AUC_{ss} and $C_{max,ss}$ exposure metrics. Each quartile includes 16 to 17 participants. A trend is observed toward higher rates of gastrointestinal (GI) disorders with an increased $C_{max,ss}$ and general

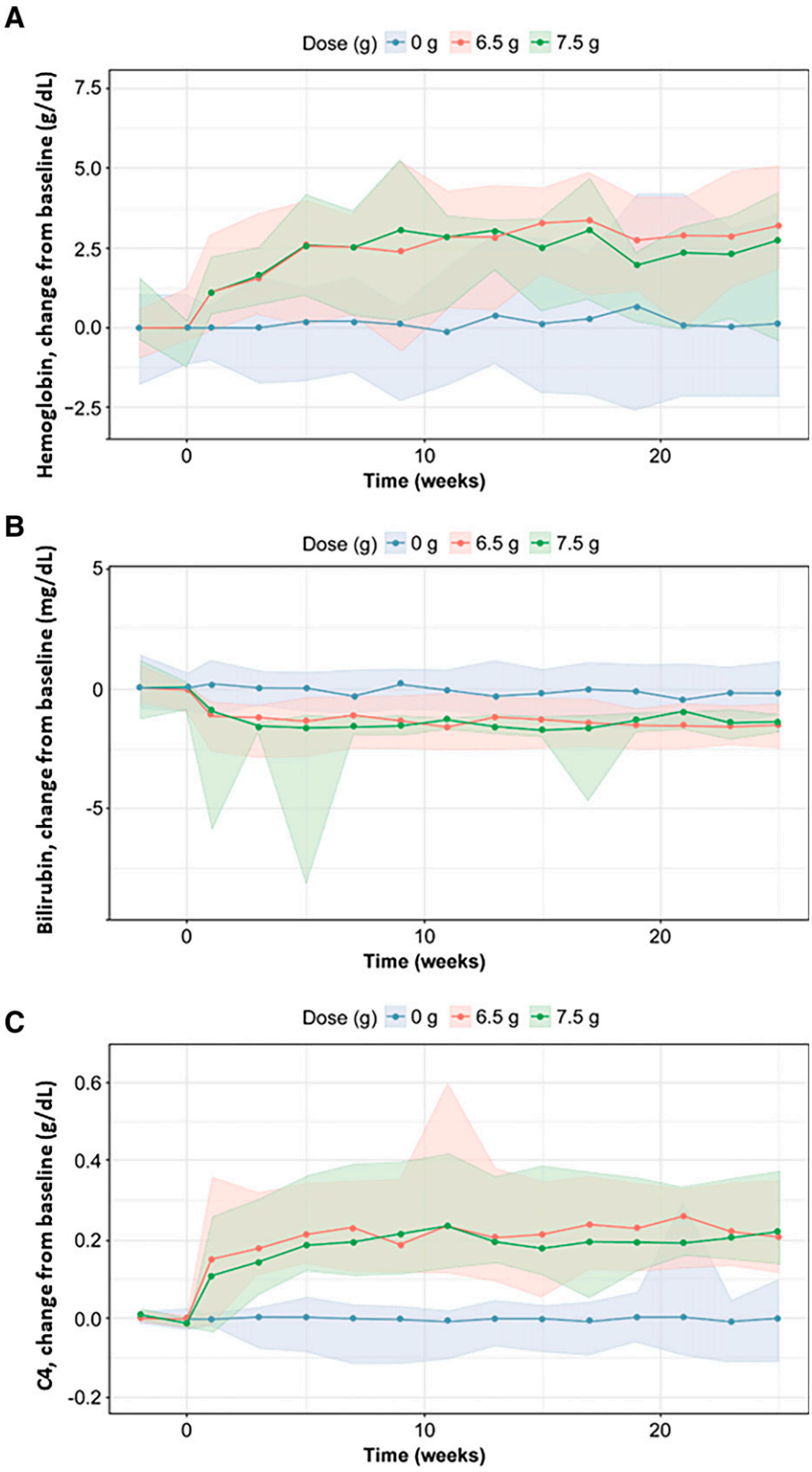

Fig. 2. Median change from baseline in hemoglobin (A), bilirubin (B), and C4 (C) over time by dose in patients with CAD (study BIVV009-04); 0 g sutimlimab (placebo) shown in blue, 6.5 g in red, and 7.5 g in green. The shaded areas represent the 2.5%–97.5% percentiles of the respective doses.

disorders and administration site reactions for AUC_{ss} and $C_{max,ss}$. The difference in percentage of patients experiencing adverse effects is between 6% and 7% between the lowest and highest AUC_{ss} or $C_{max,ss}$ quartiles for GI disorders, general disorders, and administration site discomfort. This difference is considered not relevant. In general, there does not appear to be a clear trend between the other adverse events and high exposure.

TABLE 4
Parameter estimates for the final PK/PD model

Population Parameters (Unit)	Estimate (Mean)	%RSE[a]	IIV (Mean)	%RSE[a]	η-Shrinkage (%)[b]
Baseline Hb (Hb_0, g/dl)	8.99	1.17	9.75	12.8	5.80
Effect of baseline CLCR[c] on Hb_0	0.122	36.4	ND	ND	ND
Maximum Hb effect, E_{max} logit transformation[d]	0.325	8.20	40.5	18.5	28.5
Effect of occurrence of transfusion on E_{max}[e]	−0.631	29.5	ND	ND	ND
Concentration at 50% E_{max} (EC_{50}, μg/ml)	155	48.2	ND	ND	ND
Turnover time (h)	188	16.2	ND	ND	ND
Residual variability:					
Additive residual error S.D. (g/dl)	0.916	12.0	NA	NA	

%CV, percent coefficient of variation;Hb_0, baseline Hb; NA, not applicable; ND, not determined; RSE, relative standard error.
[a]RSEs of parameter estimates are calculated as 100 × (S.E./typical value); estimates (mean) of IIV are presented as %CV; RSEs of IIV magnitude are presented on %CV scale and are approximated as 100 × (S.E./variance estimate)/2.
[b]Shrinkage (%) is calculated as 100 × (1 − S.D. of post hocs/estimated variance).
[c]Effect of baseline CLCR on Hb_0 (exponent) is relative to the median CLCR of 78.03 ml/min: $Hb_{0i} = Hb_0 (CLCR_i/78.03)^{0.122}$.
[d]Logit transform for maximum effect: $E_{max} = e^{logit}/(1+e^{logit}) = 0.245$, where logit = fixed effect parameter estimated by the model.
[e]Effect of blood transfusion on E_{max} (expressed as LOGIT) [i.e., in the presnce of at least one blood transfusion during the study LOGIT reduces to 0.173 (= LOGIT*$e^{-0.631}$)] $E_{max} = e^{logit}/(1+e^{logit}) = 0.147$.

Dose-Safety Analysis

The proportions of patients with selected safety events by dose and body weight quartiles are provided in Supplemental Results (Supplemental Figs. 14 and 15). For GI disorders, the difference in percentage of patients experiencing adverse effects is about 5% between the lowest and highest dose quartiles. For vascular disorders, the difference in percentage of patients experiencing adverse effects is about 7% between the lowest and highest weight quartiles. In general, there does not appear to be a clear trend between the other adverse events and dose or weight.

Discussion

The PK of sutimlimab was best described by a two-compartment model with parallel linear and nonlinear clearance terms (Michaelis-Menten elimination kinetics). This model adequately described the nonlinearity of sutimlimab PK especially visible at lower doses (0.3–60 mg/kg). This model also adequately described the PK of sutimlimab in patients with CAD and healthy participants.

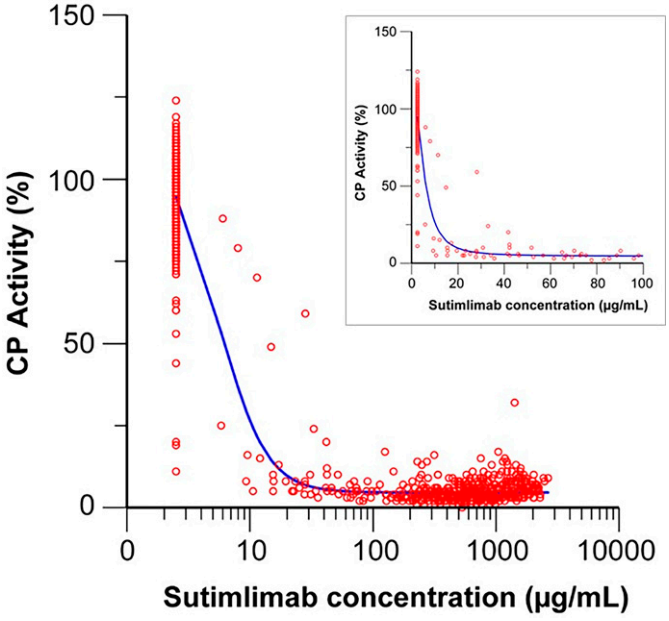

Fig. 3. Relationship between sutimlimab concentration and CP activity (parts A and B of study BIVV009-01). Circles represent the observed values, and the solid line shows the prediction. The *x*-axis on linear scale in the inset limits sutimlimab concentrations up to 100 μg/ml.

Body weight and ethnicity (Japanese) were identified as covariates on the PK of sutimlimab, signifying the importance of demographic factors in sutimlimab PK. However, other covariates such as sex, race, albumin, hepatic function, renal function, and disease status did not have an additional impact on sutimlimab PK.

Separate residual error models were used for study BIVV009-03 due to the large difference in observed concentration between steady-state dosing (BIVV009-03) and single- or multiple-dose studies. Goodness-of-fit plots indicate population predictions to deviate from observed concentrations at very low (<30 μg/ml) and very high (>5000 μg/ml) concentrations only. This is thought to be of no clinical relevance considering that maximal effects (complete CP inhibition) occur at sutimlimab levels above 20 μg/ml. Overall, there was no indication of any major model misspecification. Also, the pcVPCs confirmed concordance between observed and model-based simulations. Taken together, these suggest that the final popPK model is adequate for simulation of sutimlimab-exposure estimates in adults.

The changes of exposure parameters (i.e., $C_{min,ss}$, $C_{max,ss}$, and AUC_{ss}) at steady state in patients weighing ≥75 kg, elderly patients (age >65 years), and non-Japanese patients relative to the reference populations respectively ranged from 0.7 to 0.8, 0.8 to 1.0, and 1.2 to 1.4, respectively, altogether indicating a relatively limited impact of the previously identified covariates. Simulated concentration-time profiles using the final model showed an overlap in exposure after the 6.5-g and 7.5-g doses, indicating the that cutoff was appropriately selected. Additional simulations also showed that exposures decreased with increasing body weight and that exposures were greater in Japanese participants versus non-Japanese participants. However, minimum sutimlimab concentration at steady state was greater than the target of 100 μg/ml to prevent hemolysis, suggesting that the approved dosing regimen (6.5 g in patients <75 kg and 7.5 g in patients ≥75 kg) and dose levels provide adequate exposure in all patients-with-CAD groups. Overall, a good predictability trend of the popPK model was

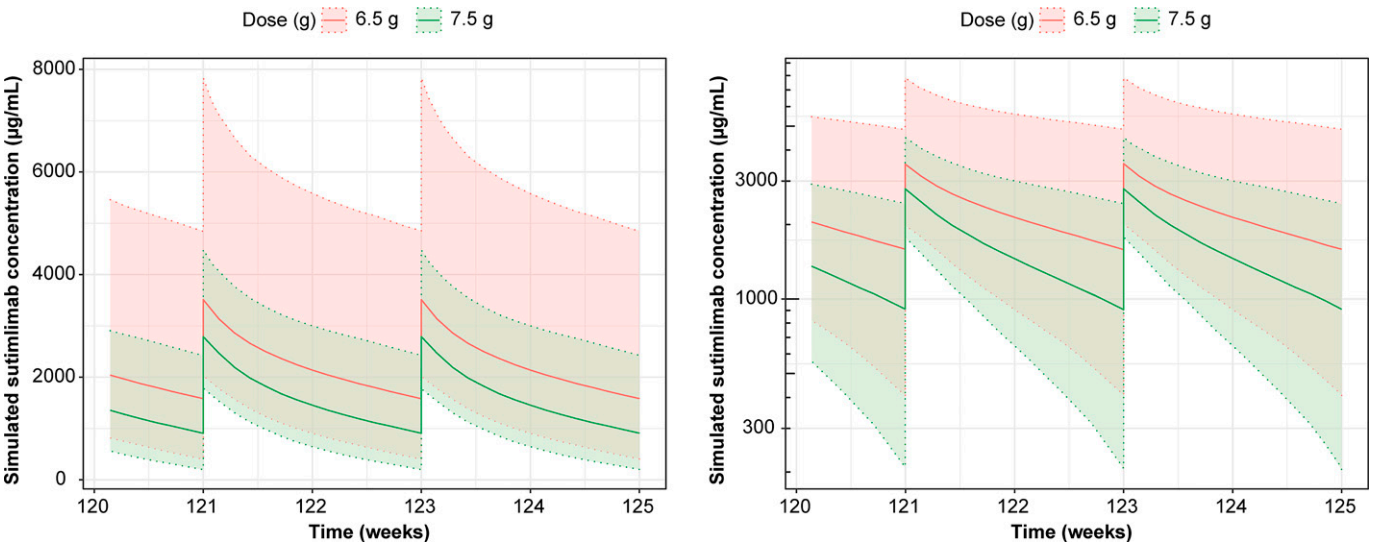

Fig. 4. Simulated concentration versus time profiles by dose after administration of 6.5 g sutimlimab to patients weighing <75 kg and 7.5 g sutimlimab to patients weighing ≥75 kg. Doses were administered on day 0, day 7, and then every 14 days thereafter through week 125. Left panel: linear scale; right panel: semilogarithmic scale; 6.5-g dose shown in red and 7.5-g dose in green. Lines represent the median, and the respective shaded areas represent the range between 5th and 95th percentiles of the simulated values. Concentration and Hb profiles at 6.5 and 7.5 g are similar and overlap.

shown consistently and successful external validation of the model was demonstrated.

The present exposure-response analysis was performed in two steps: graphical exploratory exposure-response analysis and development of a popPK/PD model for Hb. The popPK/PD model should support characterization of IIV in clinical response (Hb increase) and its explanation by covariates. Hemoglobin and C4 increased, and bilirubin was shown to decrease after administration of sutimlimab in patients with CAD in all studies. At dose of 6.5 or 7.5 g sutimlimab, the responses for Hb, C4, and bilirubin are markedly higher than those of the placebo group. Exploratory exposure-response relationship was characterized by observed $C_{min,ss}$ versus observed biomarker change. The estimated E_{max} (Hb and C4) or I_{max} (bilirubin) captured maximum observed effect on biomarkers. The estimated $C_{min,ss}$ for half-maximum effect on Hb and bilirubin (EC_{min} for Hb, IC_{min} for bilirubin) was 50.7 to 298 μg/ml with all observed $C_{min,ss}$. The result is in the same order of magnitude as the EC_{50} of the turnover model for Hb (155 μg/ml). Thus, EC_{50} is confirmed to be safely beyond 1.5–3 times the target sutimlimab $C_{min,ss}$ (100 μg/ml) to avoid breakthrough bleeds. In addition, these values are comparable to those observed in PK analyses following approved doses.

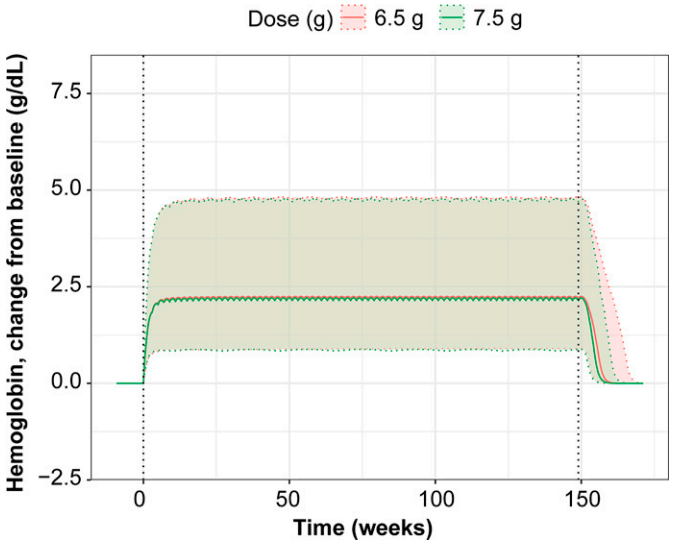

Fig. 5. Simulated Hb change from baseline versus time by dose after administration of 6.5 g sutimlimab to patients weighing <75 kg and 7.5 g sutimlimab to patients weighing ≥75 kg. Doses were administered on day 0, day 7, and then every 14 days thereafter through week 149. Figure illustrates the complete treatment period on a linear scale; 6.5-g dose shown in red and 7.5-g dose in green. The solid lines represent the median, and the respective shaded areas represent the range between 5th and 95th percentiles of the simulated values. The dotted vertical lines represent the start or end of treatment period.

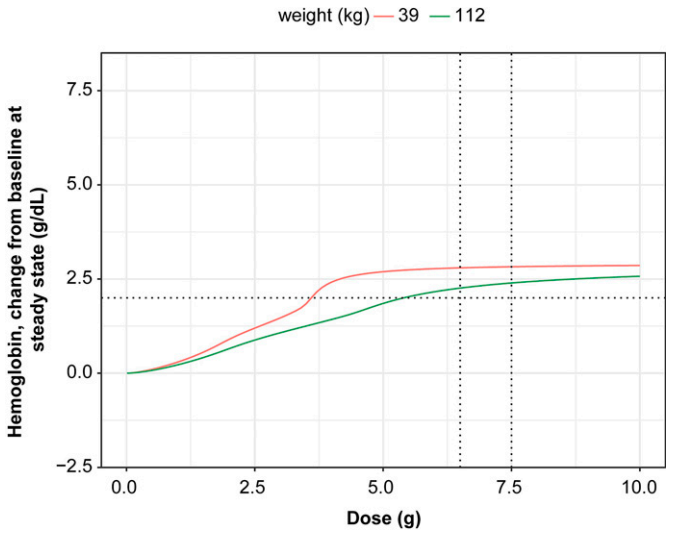

Fig. 6. Relationship between Hb change from baseline at steady state by weight (minimum and maximum weight in the population). The vertical dotted lines indicate the approved dosing: 6.5 and 7.5 g; the horizontal line represents 2 g/dl change in Hb from baseline.

The dynamic PK/PD model was an indirect response model with sutimlimab concentration inhibition of Hb turnover rate. Selection of an indirect response model was supported by hysteresis plots for time-matched observed Hb versus observed sutimlimab concentrations, which are suggestive of a time delay between sutimlimab exposure and changes in Hb response (data not shown). Integrating the turnover model with an E_{max} model to capture the drug effect is consistent with the results of the graphical exploratory analysis. The magnitude of ETA shrinkage on the IIVs was ≤30% for all PD parameters with IIV terms. In general, observations are randomly distributed around the identity line in the goodness-of-fit plots. However, low Hb measures are not captured on a population level by the model, which is reflected in the VPC, where the lower prediction interval does not capture all observations over time. The model appears to adequately predict the median change in Hb with and without treatment (i.e., change in Hb over time with placebo treatment).

The model estimated the turnover time of 188 hours with a derived median k_{out} of 0.0053 $hours^{-1}$, which corresponds to a half-life of 5.4 days. This half-life is lower than the lifetime of Hb (~120 days) but is supposed to reflect higher degradation rate of Hb in patients with CAD. The drug effect was estimated to have an E_{max} of 25% from baseline, which is in line with the projected effect of ~2 g/dl and consistent with the observations in phase 3 studies. The EC_{50} was 155 μg/ml, which is approximately 1.5 times the target sutimlimab $C_{min,ss}$ (100 μg/ml) to avoid hemolysis. The model does not contain a placebo effect (assumed as 0), which is in line with the lack of time-dependent changes observed during the exploratory analysis. Interindividual variability was identified for E_{base} and E_{max}. After stepwise covariate modeling, only CLCR and blood transfusion were kept in the model as covariates of E_{base} and E_{max}, respectively. The introduction of covariates on E_{base} and E_{max} reduced the IIV of these parameters by 12.2% and 16.5%, respectively. Patients receiving at least one blood transfusion during the study showed a lowering of E_{max} of 40%. The blood transfusion was modeled as a binary covariate (i.e., the time of the blood transfusion was not taken into account). This could contribute to the oscillations in Hb levels observed in some patients. Baseline CLCR was positively correlated with baseline Hb levels, which is consistent with current knowledge of anemia and chronic kidney disease (Hsu et al., 2002). The additive residual unknown variability was 0.92 g/dl and also reflects circadian variation of Hb levels throughout the study. This was not specifically accounted for in the model and probably at least partially explains the oscillations observed in some patients. The residual error also remained unchanged compared with the base model.

Model predictability, evaluated by means of a Bayesian analysis using predefined criteria, demonstrated that the final popPK/PD model is suitable to describe Hb data obtained from sutimlimab studies. A successful external validation of the model was also demonstrated. Deterministic simulations showed that E_{max} was attained independent of the PK (i.e., body weight, ethnicity, and age) and PD (i.e., renal function and occurrence of blood transfusion) covariate characteristics.

Given the overall low incidence of anti-sutimlimab antibodies in the BIV009-03 and BIV009-04 clinical studies (eight participants of 66 in the phase 3 studies) the effect of ADAs on sutimlimab PK and PD is considered limited, as was also confirmed by comparing plasma concentration-time profiles or PD profiles of sutimlimab for each patient. Further, no participants with confirmed treatment-emergent positive ADAs (treatment boosted or treatment induced) had treatment-emergent adverse events concerning hypersensitivity or anaphylactic reactions associated with sutimlimab.

The approved dose regimen (6.5 g for body weight <75 kg and 7.5 g for body weight ≥75 kg) was selected to maintain concentrations above 100 μg/ml in the maximum number of patients for near-maximal suppression of CP activity. The observed data from BIV009-03 and BIV009-04 studies showed that trough levels were maintained above 100 μg/ml during the treatment period without dose interruption in 90% of patients. Predicted change in Hb based on population PK/PD was maximum at the therapeutic weight tiered dose regimen (maximum Hb is more than 2 g/dl) including extreme body weight patients (39 and 112 kg).

The majority of the patients (51 of 66) from BIV009-03 and BIV009-04 studies were in the 6.5-g treated group. The dose level mean in mg/kg of the 6.5-g treatment group is 108.6 ± 18.1 mg/kg, and that of the 7.5-g treatment group is 89.7 ± 10.1 mg/kg. The mean of the dose in mg/kg overlaps between the two dose levels. The adverse events from BIV009-03 and BIV009-04 were graphically evaluated for correlation with dose (in mg/kg) or weight quartiles. No major trend was observed in adverse events with dose or body weight. In conclusion, no effect of dose (in mg/kg) or body weight on safety was observed.

In summary, the present analysis showed that the PK and PK/PD of sutimlimab can be accurately predicted using the respective models. This rigorous assessment of PK and PD data confirms the approved dosing regimen of sutimlimab, without the need for further dose adjustments in specific populations. Similar changes of Hb, bilirubin, and total C4 levels from baseline after 6.5 g or 7.5 g sutimlimab and negligible changes in the placebo group were observed. Exploratory dose/exposure-safety analyses indicate well tolerated administration with the approved dosing regimen.

Acknowledgments

The authors would like to thank the investigators, healthcare providers, research staff, volunteers, and patients who participated in the studies. Medical writing and editing support were provided by Emma East, Alex Goonesinghe, and Liz Jennings of Lucid Group Communications Ltd. This support was funded by Sanofi.

Data Availability

Qualified researchers may request access to patient-level data and related study documents, including the clinical study report, study protocol with any amendments, blank case report form, statistical analysis plan, and dataset specifications. Patient level data will be anonymized and study documents will be redacted to protect the privacy of our trial participants. Further details on Sanofi's data sharing criteria, eligible studies, and process for requesting access can be found at https://www.vivli.org/.

Authorship Contributions

Participated in research design: Frank, Kovar, Strougo, Vage, Wong.
Conducted experiments: Frank, Strougo, Vage.
Performed data analysis: Frank, Kovar, Strougo, Vage, Teuscher, Wong.
Wrote or contributed to the writing of the manuscript: Frank, Kovar, Strougo, Vage, Teuscher, Wong.

References

Bartko J, Schoergenhofer C, Schwameis M, Firbas C, Beliveau M, Chang C, Marier JF, Nix D, Gilbert JC, Panicker S, et al. (2018) A randomized, first-in-human, healthy volunteer trial of sutimlimab, a humanized antibody for the specific inhibition of the classical complement oathway. *Clin Pharmacol Ther* **104**:655–663.

Berentsen S (2016) Cold agglutinin disease. *Hematology Am Soc Hematol Educ Program* **2016**:226–231.

Berentsen S, Barcellini W, D'Sa S, Randen U, Tvedt THA, Fattizzo B, Haukås E, Kell M, Brudevold R, Dahm AEA, et al. (2020) Cold agglutinin disease revisited: a multinational, observational study of 232 patients. *Blood* **136**:480–488.

Berentsen S, Randen U, and Tjønnfjord GE (2015) Cold agglutinin-mediated autoimmune hemolytic anemia. *Hematol Oncol Clin North Am* **29**:455–471.

Broome CM, Cunningham JM, Mullins M, Jiang X, Bylsma LC, Fryzek JP, and Rosenthal A (2020) Increased risk of thrombotic events in cold agglutinin disease: a 10-year retrospective analysis. *Res Pract Thromb Haemost* **4**:628–635.

Bylsma LC, Gulbech Ording A, Rosenthal A, Öztürk B, Fryzek JP, Arias JM, Röth A, and Berentsen S (2019) Occurrence, thromboembolic risk, and mortality in Danish patients with cold agglutinin disease. *Blood Adv* **3**:2980–2985.

Chapin J, Terry HS, Kleinert D, and Laurence J (2016) The role of complement activation in thrombosis and hemolytic anemias. *Transfus Apheresis Sci* **54**:191–198.

Delvasto-Nuñez L, Jongerius I, and Zeerleder S (2021) It takes two to thrombosis: hemolysis and complement. *Blood Rev* **50**:100834.

Hsu CY, McCulloch CE, and Curhan GC (2002) Epidemiology of anemia associated with chronic renal insufficiency among adults in the United States: results from the Third National Health and Nutrition Examination Survey. *J Am Soc Nephrol* **13**:504–510 th.

Jäger U, Barcellini W, Broome CM, Gertz MA, Hill A, Hill QA, Jilma B, Kuter DJ, Michel M, Montillo M, et al. (2020) Diagnosis and treatment of autoimmune hemolytic anemia in adults: recommendations from the First International Consensus Meeting. *Blood Rev* **41**:100648.

Jäger U, D'Sa S, Schörgenhofer C, Bartko J, Derhaschnig U, Sillaber C, Jilma-Stohlawetz P, Fillitz M, Schenk T, Patou G, et al. (2019) Inhibition of complement C1s improves severe hemolytic anemia in cold agglutinin disease: a first-in-human trial. *Blood* **133**:893–901.

Kamesaki T, Nishimura J-I, Wada H, Yu E, Tsao E, Morales J, and Kanakura Y (2020) Demographic characteristics, thromboembolism risk, and treatment patterns for patients with cold agglutinin disease in Japan. *Int J Hematol* **112**:307–315.

Mühlbacher J, Jilma B, Wahrmann M, Bartko J, Eskandary F, Schörgenhofer C, Schwameis M, Parry GC, Gilbert JC, Panicker S, and Böhmig GA (2017) Blockade of HLA Antibody-Triggered Classical Complement Activation in Sera From Subjects Dosed With the Anti-C1s Monoclonal Antibody TNT009-Results from a Randomized First-in-Human Phase 1 Trial. *Transplantation* **101**: 2410–2418.

Mullins M, Jiang X, Bylsma LC, Fryzek JP, Reichert H, Chen EC, Kummar S, and Rosenthal A (2017) Cold agglutinin disease burden: a longitudinal analysis of anemia, medications, transfusions, and health care utilization. *Blood Adv* **1**:839–848.

Röth A, Barcellini W, D'Sa S, Miyakawa Y, Broome CM, Michel M, Kuter DJ, Jilma B, Tvedt THA, Fruebis J, et al. (2021) Sutimlimab in cold agglutinin disease. *N Engl J Med* **384**:1323–1334.

Röth A, Berentsen S, Barcellini W, D'Sa S, Jilma B, Michel M, Weitz IC, Yamaguchi M, Nishimura JI, Vos JMI, et al. (2022) Sutimlimab in patients with cold agglutinin disease: results of the randomized placebo-controlled phase 3 CADENZA trial. *Blood* **140**:980–991.

Address correspondence to: Dr. Thomas Frank, Sanofi-Aventis Deutschland GmbH, Industriepark Höchst, Bldg. H831, 65926 Frankfurt, Germany. E-mail: thomas.frank@sanofi.com

Supplementary materials to: '***Sutimlimab pharmacokinetics and pharmacodynamics in patients with cold agglutinin disease'***

Thomas Frank, Andreas Kovar, Ashley Strougo, Chandravathi Vage, Nathan Teuscher, and Nancy Wong

Journal of Pharmacology and Experimental Therapeutics

JPET-AR-2022-001511

Supplementary methods

Population PK model development

The base model was characterized by the following expressions:

$$C_1 = \frac{A_1}{V_2}$$

$$C_2 = \frac{A_2}{V_3}$$

$$\frac{dA_1}{dt} = -\frac{V_{max} \cdot C_1}{K_m + C_1} - CL \cdot C_1 - Q \cdot C_1 + Q \cdot C_2$$

$$\frac{dA_2}{dt} = Q \cdot C_1 + Q \cdot C_2$$

where A_1 and A_2 are the amounts of drug in the central and peripheral compartments, C_1 and C_2 the corresponding concentrations; V_2 corresponds to V_c, V_3 corresponds to V_p. V_{max}, K_m, CL, V_p, Q, and V_p were fitted. At 0 h, A_1 = dose and A_2 = 0.

The base population PK model was assessed through inclusion of inter-individual variability (IIV) terms on selected parameters. The feasibility of modelling IIV was evaluated for clearance (CL), distributional clearance (Q), central volume of distribution (V), peripheral volume of distribution

(V2), maximum non-linear clearance (V_{max}), and affinity of saturable clearance (K_m). A diagonal variance-covariance structure for the tested random effects was used at this stage of the analysis. The IIV terms were applied to the model parameters, assuming the multiplicative (proportional) form given by the expression: $\theta_{ki} = \theta_k e^{\eta ki}$, where θ_{ki} denotes the value for the k^{th} parameter for the i^{th} subject, θ_k denotes the typical value for the k^{th} parameter, and ηki denotes the IIV in the k^{th} parameter for the i^{th} subject and is assumed to have a mean of 0 and variance of ω^2.

An additive plus proportional residual error model as below was initially evaluated in the base models. Other forms of residual error models were tested to improve stability/fit, if deemed appropriate. $Y = F \times (1 + \varepsilon_1) + \varepsilon_2$ where Y is the observed data, F is the prediction based on the model, ε_1 is the proportional error component with mean of 0 and variance of σ_1^2, and ε_2 is the additive error component with mean of 0 and variance of σ_2^2.

Covariate analysis

Covariate selection was performed through iterative testing of potential covariate effects (Supp. Table 1).

Supp. Table 1. Covariates evaluated on PK parameters during model development

	PK Parameters	
Covariate	***Volume parameters***	***Clearance parameters***
Age	X	X
Body weight	X	X
Sex	X	X
Race	X	X

Japanese ethnicity (if data was available)	X	X
Disease status		X
Measures of hepatic function (albumin, AST)		X
Renal function (CRCL, eGFR)[a]		X
Presence/absence of ADAs		X

ADA, anti-drug antibody; AST, aspartate transaminase; CRCL, creatinine clearance; eGFR, estimated glomerular filtration rate; PK, pharmacokinetic.

[a]According to the Cockroft-Gault equation

During model development, the testing process consisted of stepwise forward inclusion and backward elimination. During forward inclusion, only those covariate effects that yielded an improvement in model fit that was significant at the statistical level of significance (α)=0.01 were carried forward for backward elimination testing and clinical relevance evaluation. Next, all covariate relationships incorporated into the model by the end of the forward inclusion step were subjected to backward elimination procedure with an acceptance criterion of α=0.001. In the third and final step of covariate selection, all covariates remaining in the model after the backward elimination step were further evaluated based on magnitude of impact on the parameter of interest (i.e., clinical relevance) (Supp. Table 2).

The relationships between continuous covariates and the typical value of PK parameters were modeled using power models described as follows: $\theta^i = \theta_{TV,REF}(X_i/X_{REF})^{\theta_x}$, where $\theta_{TV,REF}$ is the typical value of the PK parameter at the reference value (X_{REF}) of the continuous covariate X, θ_x is the exponent of the power covariate model, and θ_i is the individual PK parameter due to the deviation of the individual covariate Xi from X_{REF}.

The relationships between categorical covariates and the typical value of PK parameters were modeled as a multiplicative (proportional) model described as follows: $\theta i = \theta_{TV,REF} \times \theta_x{}^{X_i}$, where $\theta_{TV,\,REF}$ is the typical value of the PK parameter at the reference group of the categorical covariate X, θ_x is the proportionality constant of the covariate effect model, and θ_i is the individual PK parameter due to the individual being categorized into a group other than the reference group. X_i is the indicator variable which is equal to 1 or 0 dependent on an individual being categorized into the reference group or not.

Supp. Table 2. Covariate analysis for the PK model included in the analyses

Step	Covariates ~ PK Parameter	
Added during forward inclusion	Body weight ~ CL (ΔOFV=61)	
	Ethnicity ~ Vc (ΔOFV=55)	
	Ethnicity ~ Vmax (ΔOFV=33)	
	Body weight ~ Vc (ΔOFV=28)	
	Age ~ Vc (ΔOFV=18)	
	Age ~ Vmax (ΔOFV=6.7)	
Dropped during backward elimination	Age ~ Vmax	
Changes during model refinement[a]	Age effect on Vc between 5th and 95th percentile of Age (28 yr, 79 yr) is 19%, which is less than the a priori clinical significance minimum of 20%. Thus Age ~ Vc was removed.	
Final covariate model	Body weight effect on CL	$CL_i = \theta_{CL} * \left(\frac{Body\ weight_i}{71.85\ kg}\right)^{1.7}$
	Ethnicity effect on Vc	$V_{c_i} = \theta_{Vc} * (1 - 0.30)\ if\ Japanese$

	$V_{C_i} = \theta_{Vc}\ if\ non-Japanese$
Ethnicity effect on Vmax	$V_{max_i} = \theta_{Vc} * (1 - 0.29)\ if\ Japanese$
	$V_{max_i} = \theta_{Vc}\ if\ non-Japanese$
Body weight effect on Vc	$V_{C_i} = \theta_{Vc} * \left(\frac{Body\ weight_i}{71.85\ kg}\right)^{0.52}$

ΔOFV=change in objective function value; CL=clearance; PK=pharmacokinetic; Vc=volume of distribution of the central compartment; Vmax=maximal non-linear clearance.

a The model evaluation by MAP Bayesian approach was based on the full covariate model (including age ~V_C) to account for larger database

During model evaluation, potential new covariates were not included in the model and tested for statistical significance. Instead, individual random subject effect estimates (η) were plotted versus covariates (Supp. Table 3). Absence of covariate effect was concluded if there was no major trend.

Supp. Table 3. Covariates evaluated on PK parameters during model evaluation

	PK Parameters	
Covariate	**Volume parameters**	**Clearance parameters**
Diluted infusion	X	X
Occurrence of blood transfusion	X	X
Disease status	X	X
Presence/absence of ADAs	X	X

ADA, anti-drug antibody; PK, pharmacokinetic.

Population PK-PD model development

An E_{max} model related the Hb-increasing effect of sutimlimab to the sutimlimab plasma exposure at time t using the following equations:

$$\frac{dHb(t)}{dt} = k_{in} - k_{out} \cdot [1 - Ef_c] \cdot Hb(t)$$

$$Ef_{C,d} = E_{max} \frac{C(t)}{C(t) + EC_{50}}$$

$$Ef_{C,p} = 0$$

where Hb(t) is the Hb at time t, k_{in} and k_{out} are rate parameters related to Hb production/elimination, C(t) is the concentration of sutimlimab at time t, Ef_C is the effect as a function of the individual predicted drug concentration units, $Ef_{C,d}$ describes the Hb-elevating effect of sutimlimab, $Ef_{C,p}$ the placebo effect, E_{max} is the maximal increase in Hb, and EC_{50} is the concentration required to reach 50% of Emax.

The turnover rate parameters were estimated:

$$k_{out} = \frac{1}{Turnover}$$

$$k_{in0} = Hb(0) \cdot k_{out}$$

$$E_{max} = \frac{e^{\theta}}{(1 + e^{\theta})}$$

where k_{in0} is the baseline value of k_{in} and Hb(0) is the baseline level of Hb. The E_{max} was restricted between 0 and 1 through a log transformation.

Supp. Fig. 1: Illustration of the final sutimlimab PK/PD model structure

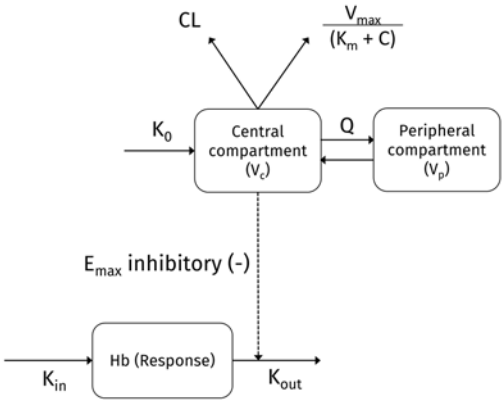

Supp. Fig. 1: A dynamic popPK/PD structural model for Hb was developed by linking the complete time profile of sutimlimab concentrations to the time profiles of Hb. The PD component was based on an indirect response/turnover model for Hb dynamics over time, including a zero-order rate constant (k_{in}) for Hb production, and a first-order rate constant (k_{out}) for elimination of Hb, which is inhibited by sutimlimab concentration in the central compartment (C).
CL, clearance; K_m, concentration required for half-maximal non-linear clearance; K_0, infusion rate; Q, inter-compartmental clearance; V_c, volume of distribution of the central compartment; V_{max}, maximal non-linear clearance; V_p, volume of distribution of the peripheral component.

Statistical models

The random effects of pop PK/PD included IIV. The distribution of the parameters was assumed log-normal, so that exponential models were used to account for IIV: $P_i = TVP \cdot e^{\eta_i}$, where P_i is the estimated parameter value for a given individual *i, TVP* is the typical population value of the parameter, η_i describes the variation of individual *i* from the population estimate. In all cases, η is assumed to be normally distributed: $\eta_i \sim N(0, \omega^2)$, with inter-individual variance-covariance matrix Ω.

The statistical model for residual variability defines the nature of the interaction between the error and the predicted value to yield the observed value. The difference between the j^{th} observed value (Y) in the i^{th} individual and its respective prediction (F) was modeled with an additive error model: $Y_{ij} = F_{ij} + \varepsilon_{i,j}$. The $\varepsilon i,j$ are independent, identically distributed statistical errors with a mean of 0 and a variance of σ^2. The additive model for residual variability assumes that the variance of observations remains constant with the predicted values and the estimate is expressed as a standard deviation (σ).

Covariate analysis

Plots of IIV versus covariates defined in Supp. Table S4 were used to screen for factors that affect sutimlimab PD. For continuous covariates, scatter plots of η (IIV code used in NONMEM) versus covariates were overlaid with a non-parametric locally weighted smoother Loess line to determine functional relationships. Only those PK/PD model parameters were considered where IIV could be estimated (i.e., E_{base} and E_{max}). For categorical covariates, box-and-whisker plots were used to identify potential differences between groups. A clear trend of positive or negative slopes and noteworthy correlation coefficients would suggest a possible influence by the continuous covariates; pronounced differences among the groups would suggest a possible influence by the categorical covariates. The plot of ηE_{base} versus potential categorical covariates suggested an influence of occurrence of at least one blood transfusion during study on the baseline Hb level estimated by the model. The plot of ηE_{base} versus potential continuous covariates suggested an influence of baseline CLCR and alanine transaminase (ALT) on the baseline Hb level estimated by the model.

With regard to E_{max}, the plot of ηE_{max} versus potential categorical covariates suggested an influence of occurrence of at least one blood transfusion during study and sex on E_{max}, and an influence of baseline ALT.

Covariate analysis was performed at the level of the base model (combined structural and statistical model) considering only variables with a clear trend seen in graphical evaluation. The covariates (Supp. Table 4) were evaluated using the stepwise covariate modeling procedure in NONMEM (same criteria as for popPK model). The investigational model for continuous and categorical covariates are shown below, where COV_i represents the individual covariate.

$$log(TVP) = log(\theta_x) + log\left(\frac{COV_i}{\text{Median}_{\text{COV}_i}}\right) \cdot \theta_y$$

$$log(TVP) = \begin{cases} log(\theta_x) + 0 & if\ COV_i = 0 \\ log(\theta_x) + COV_i \cdot \theta_y & if\ COV_i = 1 \end{cases}$$

Supp. Table 4. Covariates evaluated on PD parameters

Covariate	**E_{base}**	**E_{max}**
Age	X	X
Body weight	X	X
Sex	X	X
Race	X	X
Japanese ethnicity (if data was available)	X	X
Renal function (CRCL, eGFR)[a]	X	X
Measures of hepatic function (albumin, AST, ALT)	X	X
Presence/absence of ADAs	X	X
Occurrence of blood transfusion	X	X
Infusion dilution	X	X
Baseline Hb	X	X
Baseline bilirubin	X	X

[a]According to the Cockroft-Gault equation.

ADA, anti-drug antibodies; ALT, alanine transaminase; AST, aspartate transaminase; CLCR, creatinine clearance; E_{base}, baseline level of Hb; E_{max}, maximum effect; eGFR, estimated glomerular filtration rate; Hb, hemoglobin; PD, pharmacodynamic.

Model evaluation

Goodness-of-fit plots

Goodness-of-fit was graphically evaluated. The observed sutimlimab concentrations versus predicted concentrations, and observed Hb versus predicted Hb, were investigated to determine if the model described the data accurately. The descriptive performance of the models was also evaluated by calculation of normalized prediction distribution errors (NPDE). The NPDE should follow a $\mathcal{N}(0, 1)$ distribution, and statistical tests were used to evaluate significant differences from the theoretical $\mathcal{N}(0, 1)$ distribution.

Quality criteria

The measured (observed) concentrations (DV) and the corresponding predicted concentrations (PRED and IPRED) were evaluated in terms of mean prediction error (MPE; bias), root mean squared error; (RMSE; precision), and absolute average fold error (AAFE) using the following formulas:

$$MPE = \frac{1}{n}\sum_{i=1}^{i=n}[(I)PRED_i - DV_i]$$

$$RMSE = \sqrt{\frac{1}{n}\sum_{i=1}^{i=n}[(I)PRED_i - DV_i]^2}$$

$$AAFE = 10^{\frac{\sum_{i=1}^{i=n}\left|\log_{10}\frac{(I)PRED_i}{DV_i}\right|}{n}}$$

Where IPRED is the dividual predicted data based on individual empirical Bayes parameter estimates and PRED is the predicted data based on population parameter estimates (η = 0). MPE and RMSE are also expressed as a percentage of the mean observed concentration value (DV):

$$\text{MPE\%} = \frac{1}{n}\sum_{i=1}^{i=n}[(I)PRED(i) - DV(i)] \cdot \frac{100}{\overline{DV}}$$

$$RMSE\% = \sqrt{\frac{1}{n}\sum_{i=1}^{i=n}[(I)PRED(i) - DV(i)]^2} \cdot \frac{100}{\overline{DV}}$$

Visual predictive check (VPC)

In the prediction corrected (pc) VPC, the observed and simulated data are normalized using the population prediction:

$$pcY_{i,j} = Y_{i,j} \cdot \frac{\overline{PRED_{bin}}}{PRED_{i,j}}$$

$Y_{i,j}$ and $pcY_{i,j}$ denote the simulated data of the j^{th} observation for the i^{th} individual and the respective prediction-corrected value. The parameter $PRED_{i,j}$ is the population prediction considering the independent and design variables and sampling time j of the i^{th} individual. $PRED_{bin}$ is the median of the population prediction of all observations in the respective bin. The same prediction-correction is applied for the observed measurements ($y_{i,j}$).

Exposure parameters

The $C_{min,ss}$, $C_{max,ss}$, and $AUC_{,ss}$ at steady state were estimated for each subject included in this analysis considering dosing schedule and regimen as defined in studies 903 and 904. Calculations were performed in R using the prior model structure and the individual post hoc estimates from NONMEM model. Steady state was assumed to be attained after 100 weeks. $AUC_{,ss}$ was calculated using the trapezoidal rule and $C_{min,ss}$ was the estimated sutimlimab

concentration 1 hour prior to the next dose administration at steady state. $C_{max,ss}$ was the maximum concentration occurring in this interval at the end of infusion. The steady state $C_{min,ss}$, $C_{max,ss}$, and $AUC_{,ss}$ ratios relative to the reference population were calculated by dividing the individual post hoc estimates of $C_{min,ss}$, $C_{max,ss}$, and $AUC_{,ss}$ by the respective reference population mean $C_{min,ss}$, $C_{max,ss}$, or $AUC_{,ss}$. The reference populations were: patients weighing <75 kg, elderly patients (age >65 years) and non-Japanese patients.

The $C_{min,ss}$, $C_{max,ss}$, and $AUC_{,ss}$ values were summarized by descriptive statistics. Boxplots were used to visualize $C_{min,ss}$, $C_{max,ss}$, and $AUC_{,ss}$ versus dose (6.5 and 7.5 g), grouped by study and by previously identified covariates including occurrence of blood transfusion and excluding race and creatinine clearance. Forest plots trellised by dose group were used to visualize the mean and 95% CI of the change in $C_{min,ss}$, $C_{max,ss}$, and $AUC_{,ss}$ at steady state relative to the reference population.

Handling of missing or erroneous data

Concentration samples missing corresponding dosing data were excluded from the analysis, as were samples with missing time or date information. Concentration samples below the lower limit of quantification (LLOQ) were treated as missing and excluded from the analysis. If more than 10% of the data were below the LLOQ, likelihood-based methods of imputation, (e.g., M3 likelihood imputation) were considered. When the value of a continuous demographic covariate was missing for an analysis subject, the median value from the rest of the population was used as the imputed value. Missing categorical covariates were flagged with an appropriate missing value code in the analysis dataset (i.e., -99), but grouped together with the most common covariate category during covariate model building.

Outliers were excluded from model-building, particularly during the covariate testing phase. Prior to model-building, exploratory graphical analysis was used to identify unusual patterns and/or data points. Initial runs of the base population PK model were used to flag potential outlier values. Data observations for which the absolute value of the associated conditional weighted residual was greater than 4 (|CWRES| >4) were flagged as “questionable outliers”. These values did not create undue model destabilization or PK parameter changes and were not excluded from the analysis. The final population PK model was run using the entire dataset.

Missing variables were excluded by setting missing dependent variable (MDV) to 1. Biomarker values/sutimlimab concentrations below the LLOQ or which were flagged as missing were excluded from the analysis by setting MDV to 1. Duplicated records, Hb data with abnormally high (>25 g/dL) or low values (<1 g/dL), and post-dose concentrations without preceding dose records were excluded from the analysis by setting MDV to 1. Records with missing doses or missing treatment assignments were deleted from the dataset.

Supplementary results

Supplementary Results Tables

Supp. Table 5. Quality criteria for PK model

Criteria	Parameter	n	Value [µg/mL]	95% CI (Lower bound)	95% CI (Upper bound)	Value (% Observed)	AAFE
MPE	PRED	4140	-20.0	-43.3	3.28	-1.18	1.37
MPE	IPRED	4140	-26.7	-40.7	-12.8	-1.58	1.17
RMSE	PRED	4140	764	726	800	45.2	NC
RMSE	IPRED	4140	458	431	484	27.1	NC

AAFE, absolute average fold error; CI, confidence interval; IPRED, individual predicted data based on individual empirical Bayes parameter estimates; MPE, mean prediction error; NC, not computed; PK, pharmacokinetic; PRED, predicted data based on population parameter estimates ($\eta = 0$); RMSE, root mean squared error.

Supp. Table 6. Quality criteria for PK/PD model

Criteria	Parameter	n	Value [g/dL]	95% CI (Lower bound)	95% CI (Upper bound)	Value (% Observed)	AAFE
MPE	PRED	4269	-0.197	-0.245	-0.150	-1.76	1.12
MPE	IPRED	4269	0.001	-0.030	0.032	0.013	1.07
RMSE	PRED	4269	1.61	1.57	1.64	14.4	NC
RMSE	IPRED	4269	1.04	0.996	1.07	9.24	NC

AAFE, absolute average fold error; CI, confidence interval; IPRED, individual predicted data based on individual empirical Bayes parameter estimates; MPE, mean prediction error; NC, not

computed; PD, pharmacodynamic; PK, pharmacokinetic; PRED, predicted data based on population parameter estimates (η = 0); RMSE, root mean squared error.

Supp. Table 7. Predicted proportion of CAD patients with trough concentrations below 100 µg/mL and 20 µg/mL (n =50; 200 replicates) using proposed body weight distributions

Regimen	Weight group	Median trough concentration (µg/mL)	90% PI Lower	90% PI Upper	Mean % below 100µg/mL (90% PI)	Mean % below 20 µg/mL (90% PI)
5.5 g	< 45 kg	1730	136	3260	2.80 (0 – 27.5)	2.90 (0 – 12.5)
	≥45 to < 55 kg	1310	6.33	2690	5.70 (0 – 25.4)	7.00 (0 – 15.2)
	≥55 to < 65 kg	913	4.27	2020	7.90 (0 – 25.0)	18.5 (0 – 41.7)
	≥65 to < 75 kg	628	1.28	1540	11.8 (0 – 28.6)	1.40 (0 – 10.0)
	≥75 to < 85 kg	446	0.592	1190	17.4 (0 – 42.9)	4.20 (0 – 10.3)
	≥85 to < 95 kg	335	0.248	926	23.5 (0 – 50.0)	13.1 (0 – 33.3)
	≥95 kg	160	0.00472	635	39.3 (14.2 – 66.7)	1.10 (0 – 9.1)

	All	516	0.445	1870	17.7 (10.0 – 26.0)	11.9 (6.0 – 20.0)
75 mg/kg	< 45 kg	221	0.307	1310	41.4 (0 – 100.0)	36.2 (0 – 100.0)
	≥45 to < 55 kg	393	0.403	1330	31.8 (0 – 66.7)	26.3 (0 – 66.7)
	≥55 to < 65 kg	518	0.778	1430	20.8 (0 – 50.0)	16.1 (0 – 37.6)
	≥65 to < 75 kg	553	0.926	1390	14.1 (0 – 33.3)	10.2 (0 – 27.3)
	≥75 to < 85 kg	563	1.39	1360	12.4 (0 – 33.3)	8.40 (0 – 27.3)
	≥85 to < 95 kg	571	13.2	1270	9.20 (0 – 33.3)	5.40 (0 – 25.0)
	≥95 kg	472	3.53	1150	11.0 (0 – 33.3)	6.40 (0 – 22.2)
	All	516	0.859	1340	16.0 (8.00 – 24.1)	11.7 (4.00 – 20.0)
6.5 g for <75 kg 7.5 g for ≥75 kg	< 45 kg	2490	700	4280	2.40 (0 – 0)	1.20 (0 – 0)
	≥45 to < 55 kg	1880	426	3590	2.10 (0 – 17.0)	1.60 (0 – 16.7)
	≥55 to < 65	1330	215	2650	4.10 (0 – 16.7)	3.30 (0 – 14.3)

	kg					
	≥65 to < 75 kg	950	67.8	1980	5.50 (0 – 20.0)	4.40 (0 – 16.7)
	≥75 to < 85 kg	908	197	1900	3.40 (0 – 14.4)	2.40 (0 – 12.5)
	≥85 to < 95 kg	715	84.9	1590	5.10 (0 – 22.2)	3.00 (0 – 14.3)
	≥95 kg	365	0.313	1090	16.6 (0 – 42.9)	9.10 (0 – 33.3)
	All	907	55.8	2500	6.20 (2.00 – 12.0)	4.00 (0 – 8.00)

PI: prediction interval.

Supplementary Results Figures

Supp. Fig. 2. Goodness of fit plots for the PopPK model.

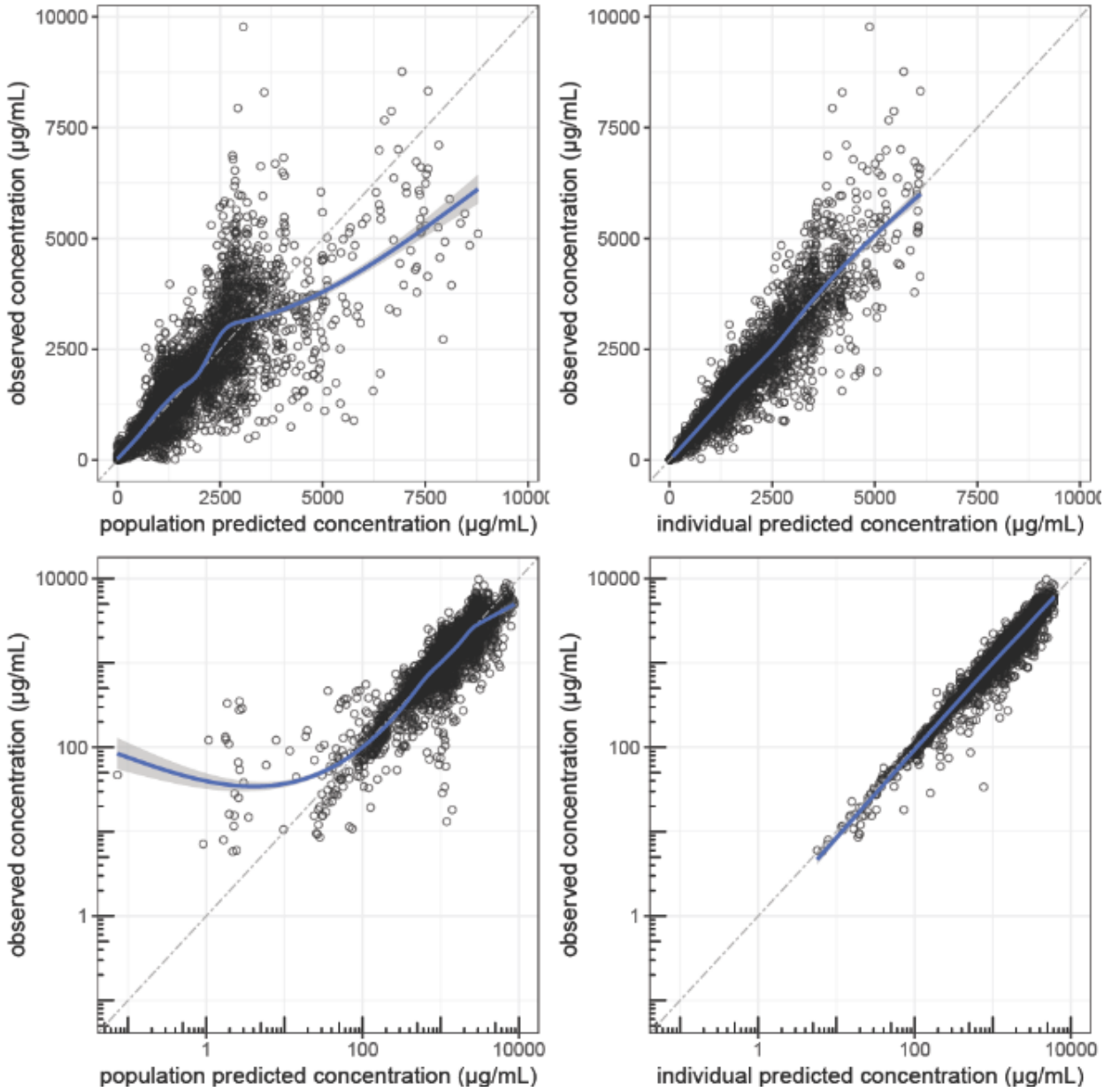

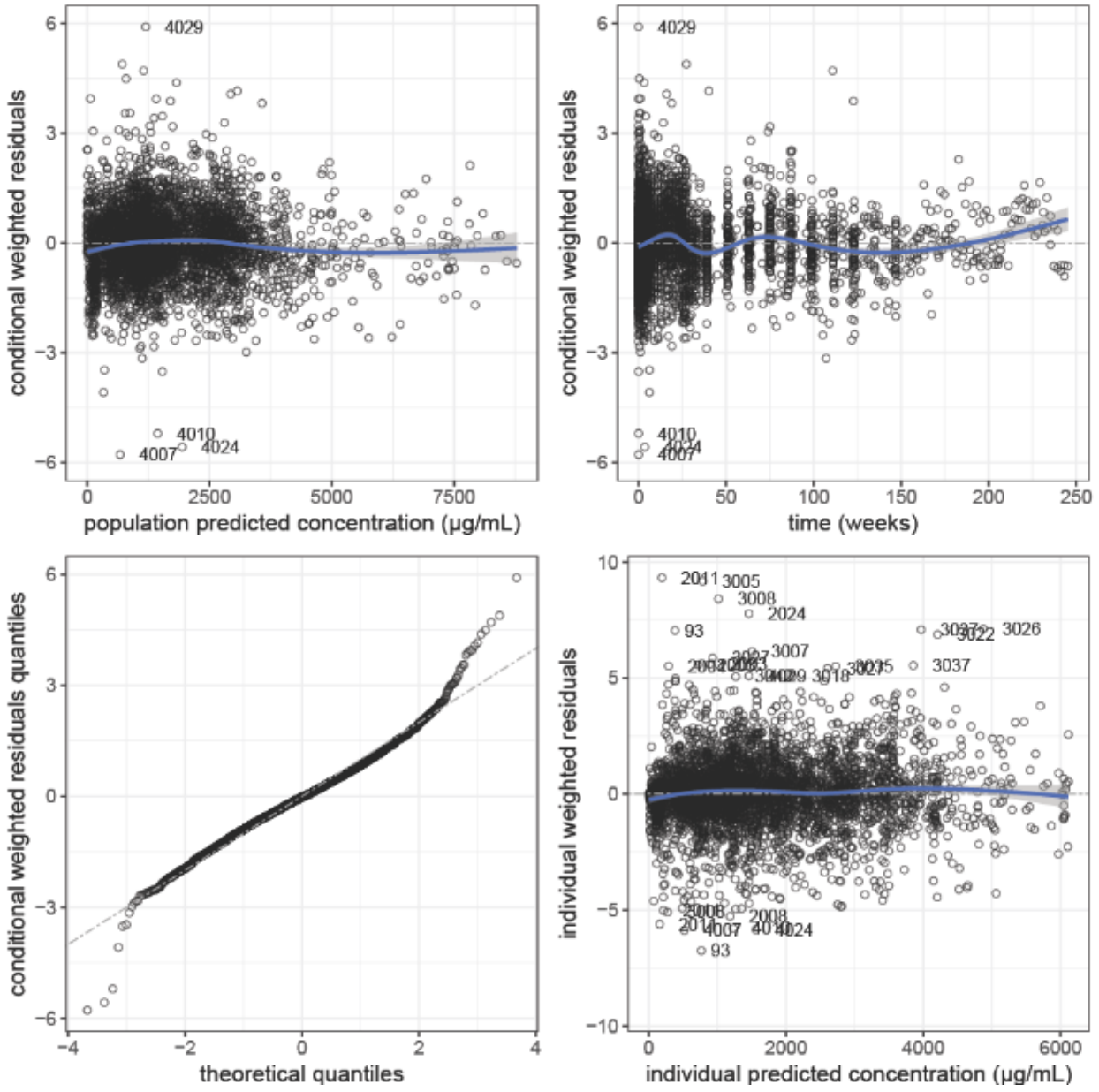

Supp. Fig. 2: The dashed line represents the identity line or zero line; the thick blue curve is the smoothing spline. Numbers indicate subject numbers with weighted residuals greater than 5 or less than -5.

PopPK, population pharmacokinetic.

Supp. Fig. 3. Prediction-corrected visual predictive check plot of final popPK model

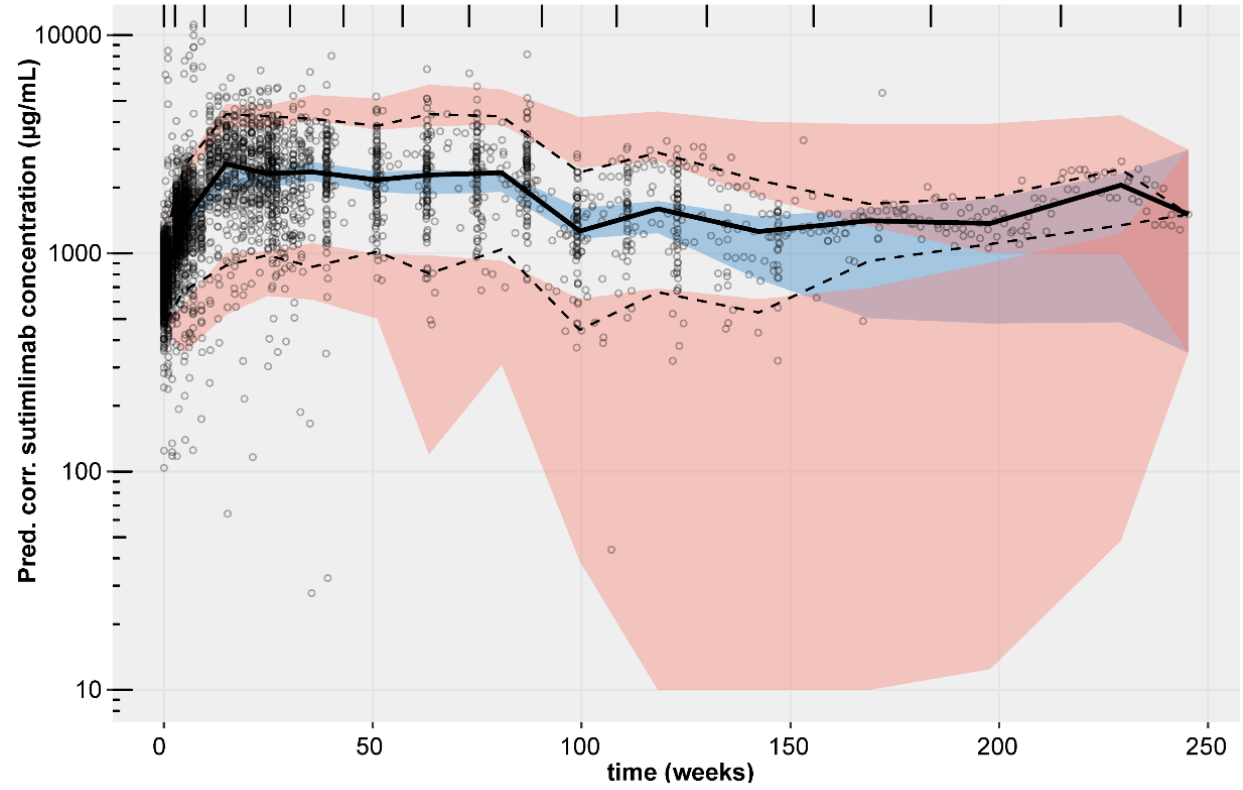

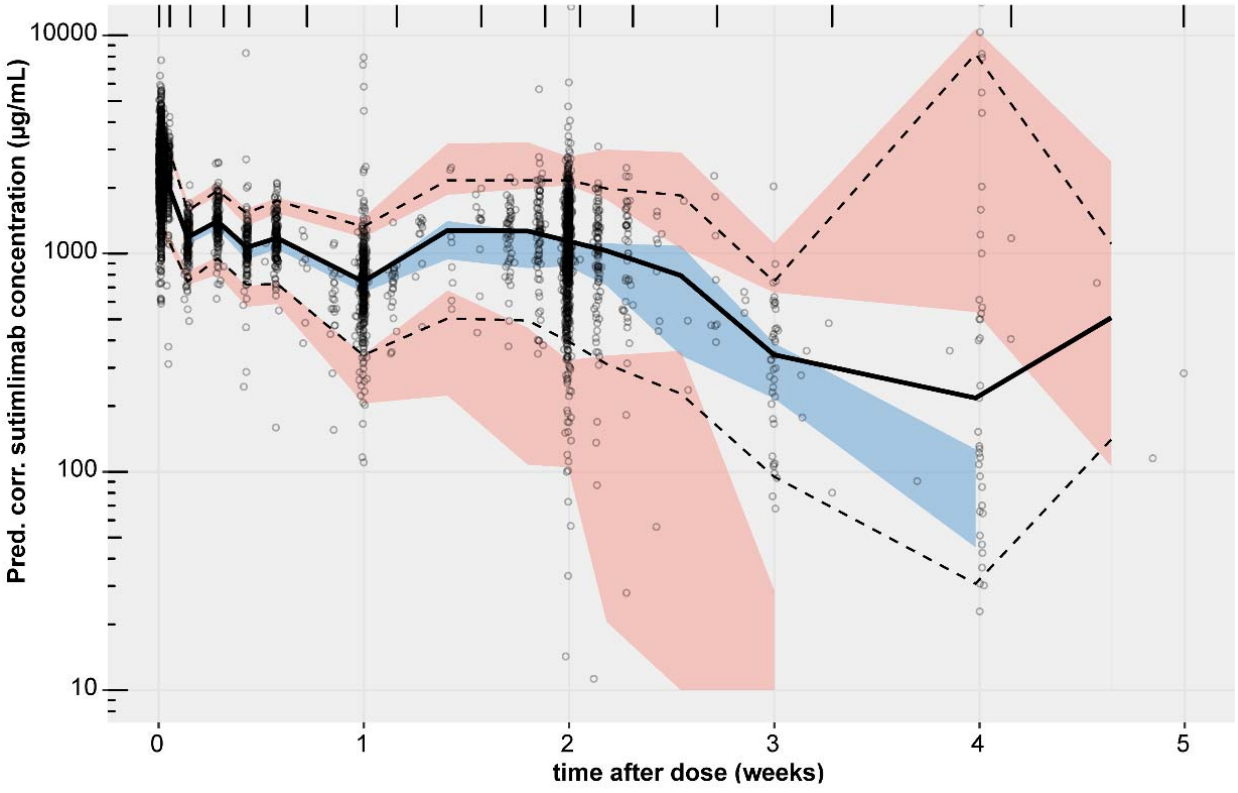

Supp. Fig. 3: The solid line represents the 50% percentile (median) of the observations. The observed 5% and 95% percentiles are presented with dashed lines. The shaded areas represent the 90% confidence interval around the 5%, 50% (median) and 95% percentiles of the simulations (n = 500 subproblem simulations).

popPK, population pharmacokinetics.

Supp. Fig. 4. Prediction-corrected visual predictive check plot for CAD patients (upper panel, Study BIVV009-03, lower panel, study BIVV009-04)

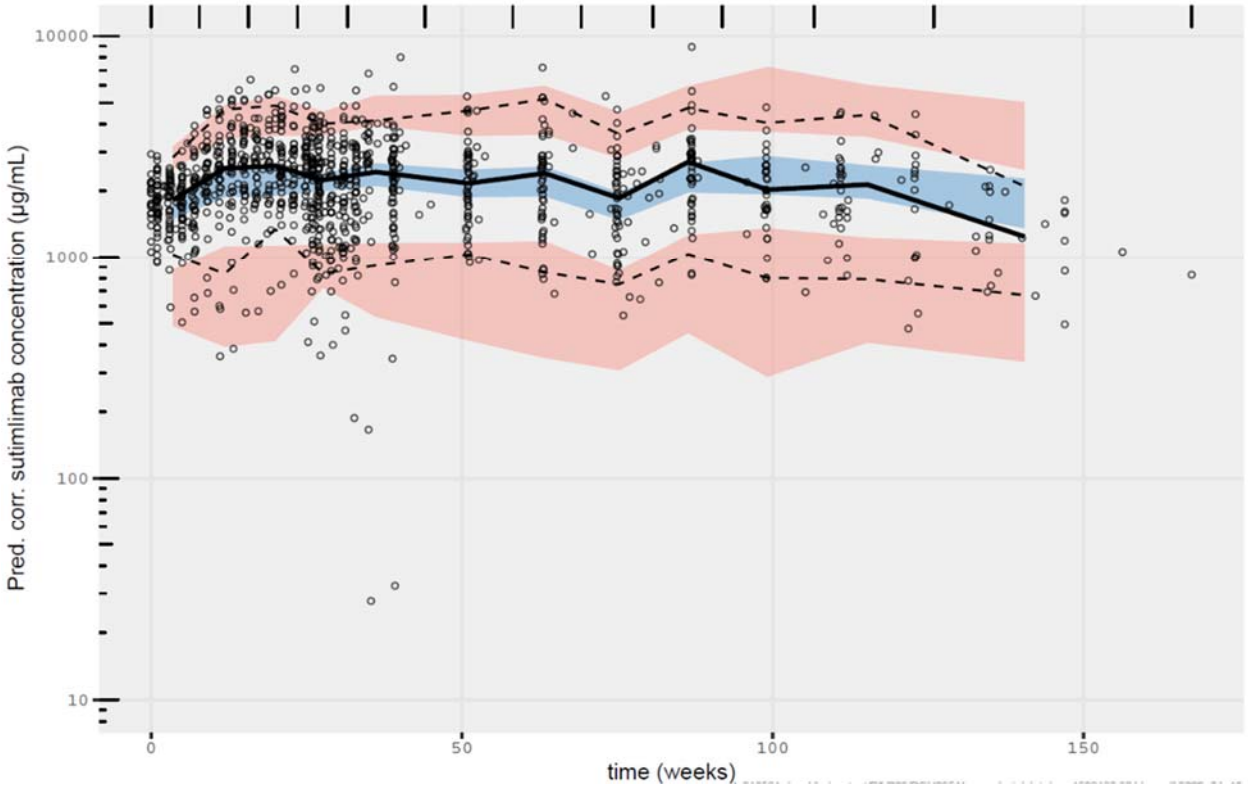

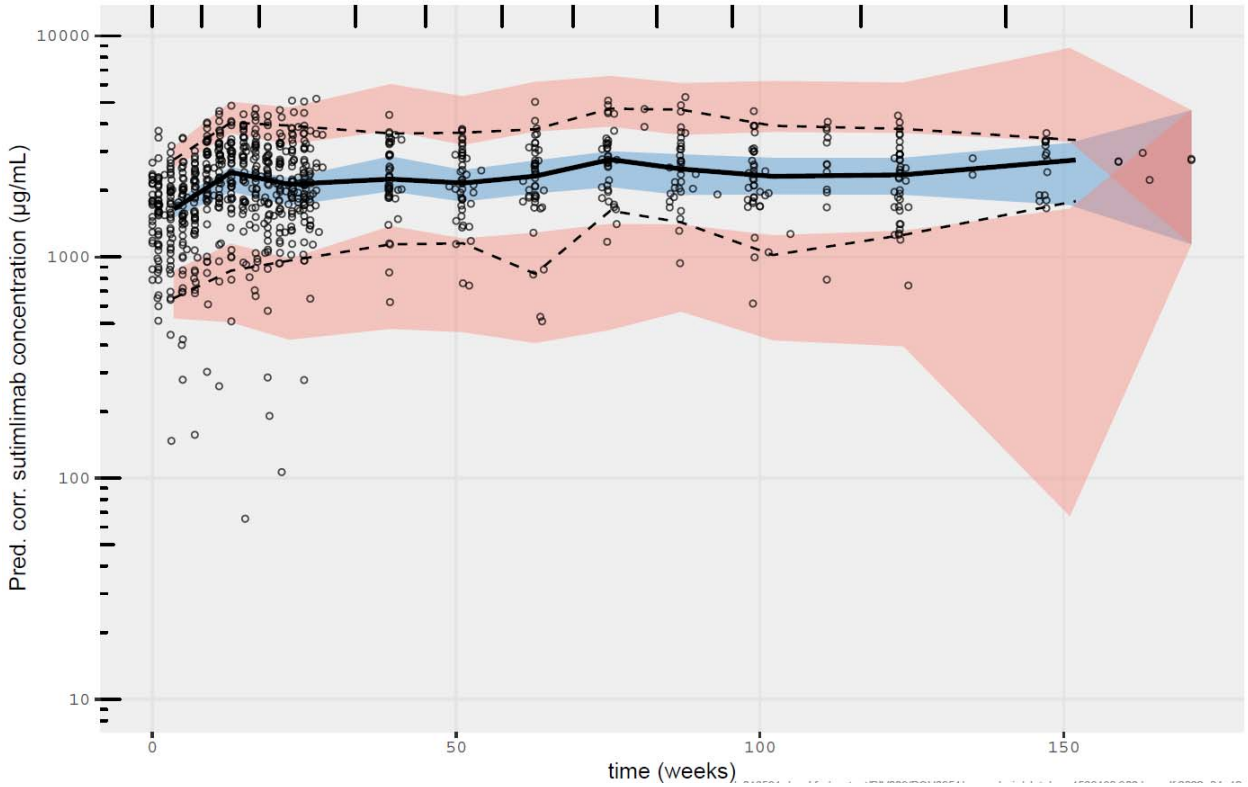

Supp. Fig. 4: Dots represent observations. The solid line represents the 50% percentile (median) of the observations. The observed 5% and 95% percentiles are presented with dashed lines. The shaded areas represent the 90% confidence interval around the 5%, 50% (median) and 95% percentiles of the simulations (n = 500 subproblem simulations)

Supp. Fig. 5. Normal Q-Q plot of NPDE, plot of NPDE vs time and PRED, and histogram of NPDE with the probability density function of the overlaid standard Gaussian distribution.

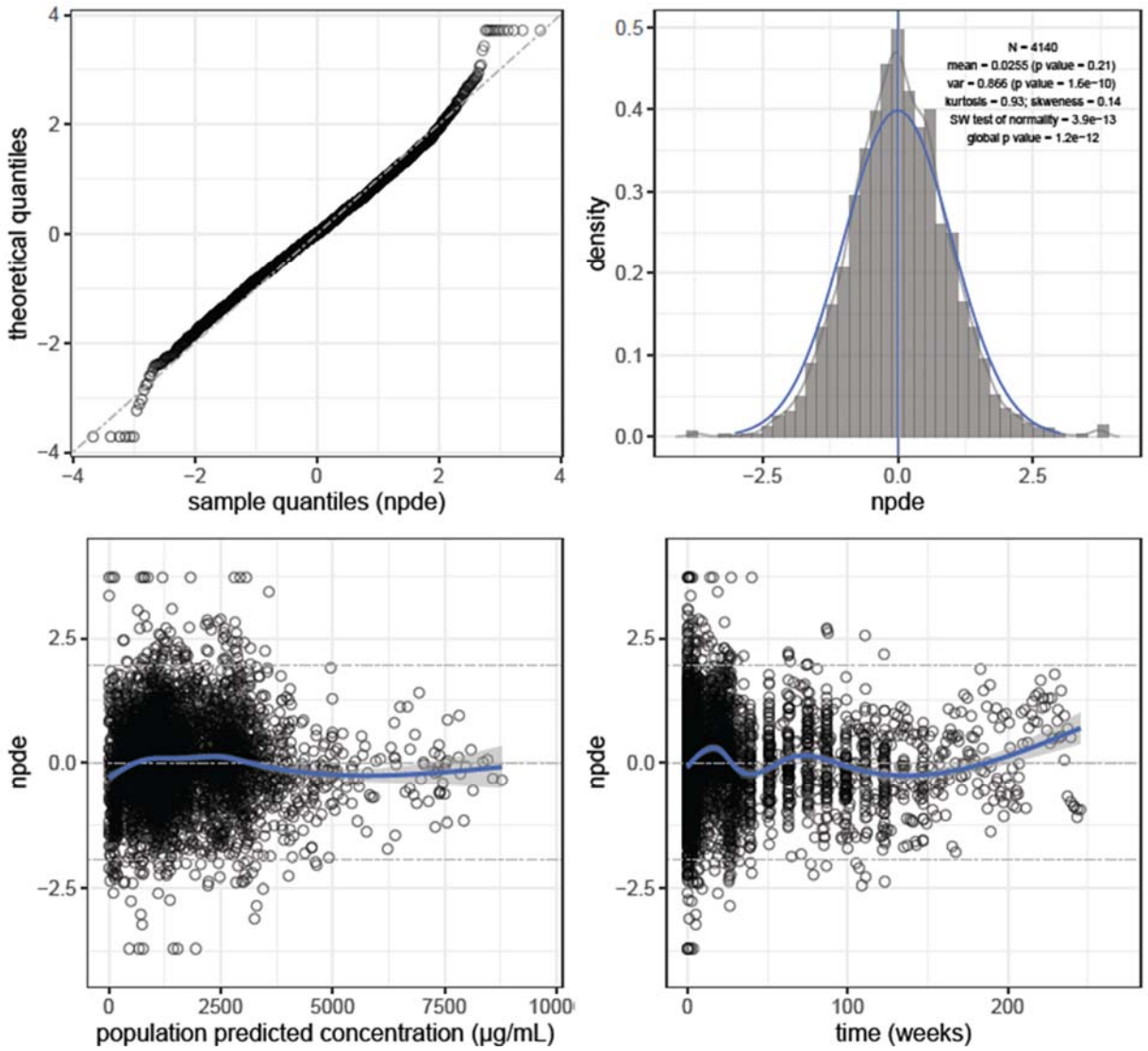

Supp. Fig. 5: The dashed line represents the identity line in Q-Q plot or the range between -1.96 and 1.96 in the plot of NPDE vs time and PRED; the thick blue curve is the smoothing spline. NPDE, normalized prediction distribution errors; PRED, predicted data based on population parameter estimates; Q-Q, quantile-quantile.

Supp. Fig. 6. Exposure-response of all observed $C_{min,ss}$ versus time matched observed hemoglobin change (a), bilirubin change (b), and C4 change (c) from baseline in patients with CAD

(a)

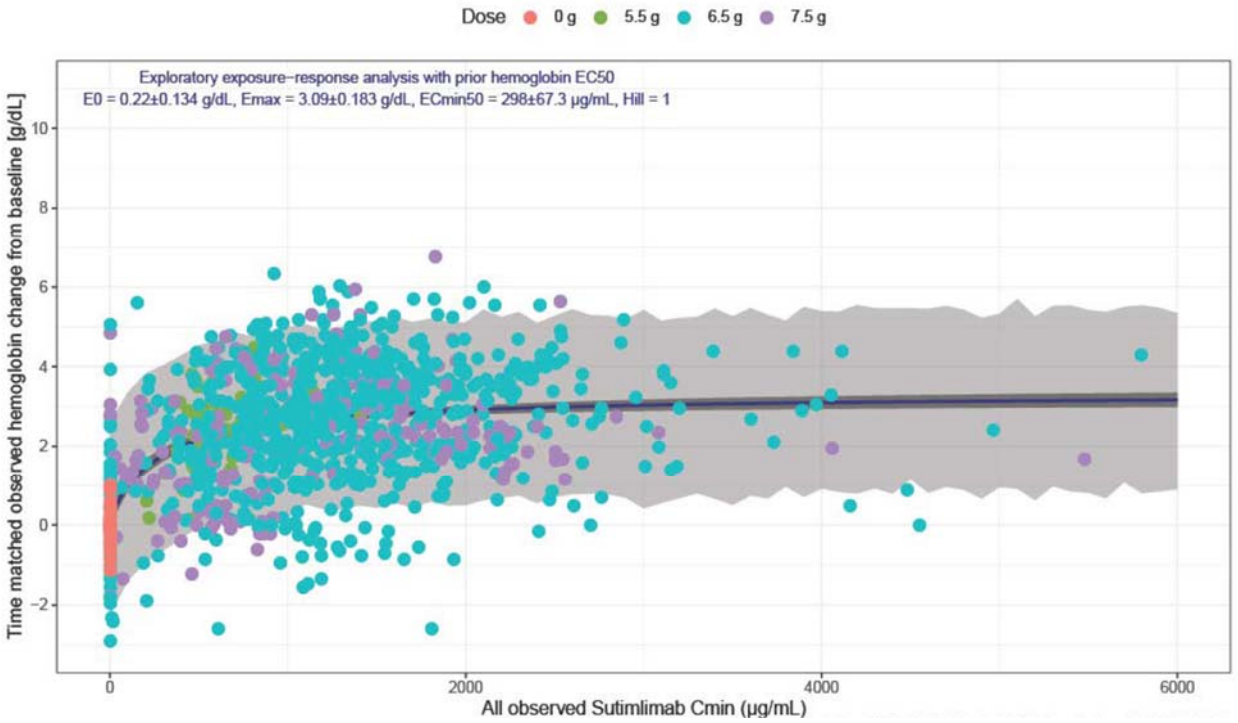

(b)

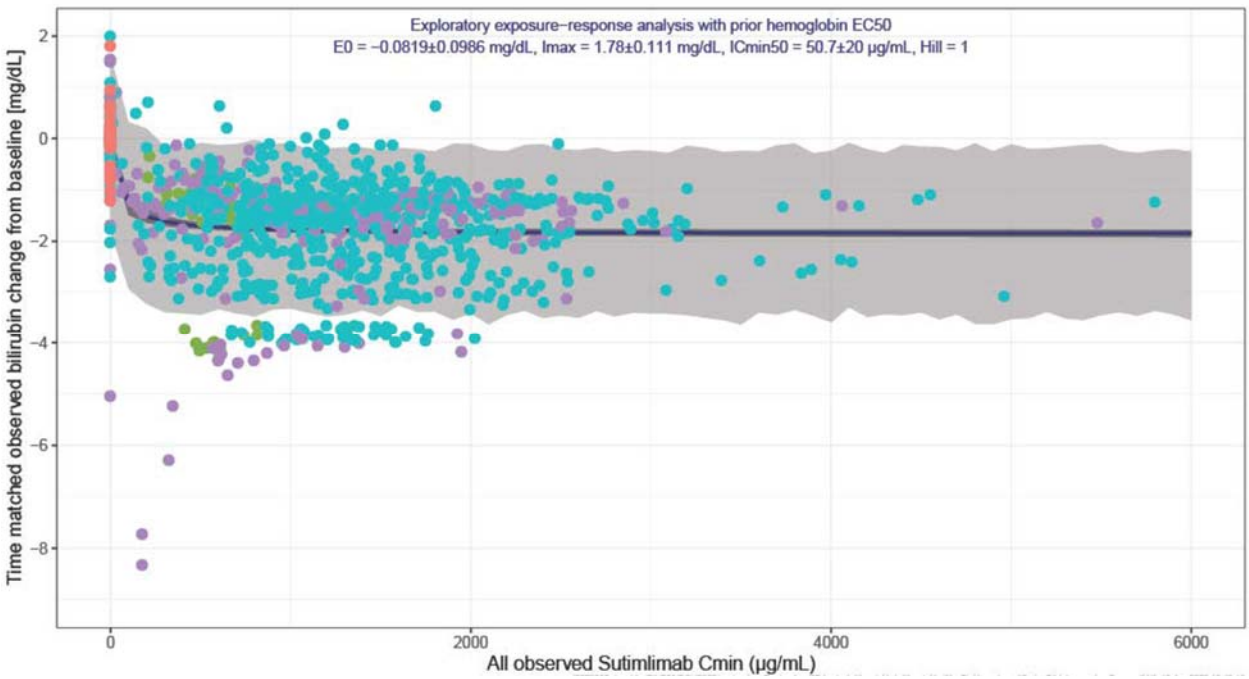

(c)

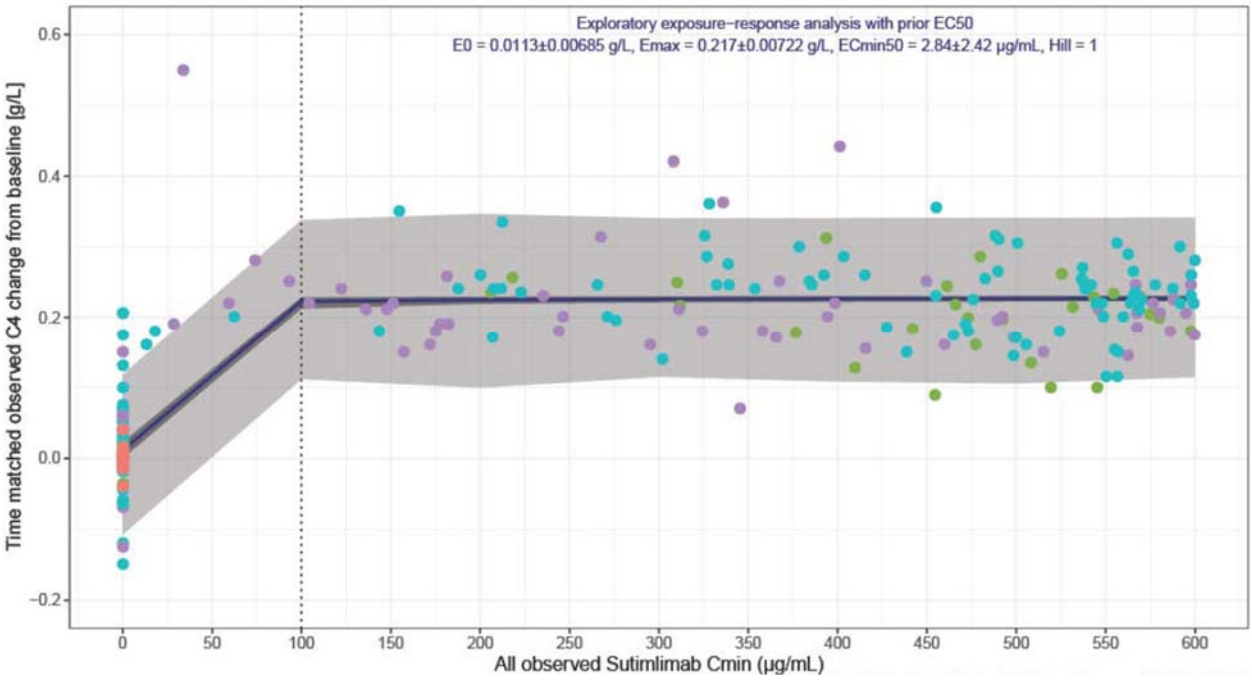

Supp. Fig. 6: Symbols represent observations; dark band represents the 90% confidence interval of the typical prediction; light band represents the 90% prediction interval.

CAD, cold agglutinin disease; $C_{min,ss}$, minimum concentration.

Supp. Fig. 7. Goodness of fit plots for the PopPK/PD model.

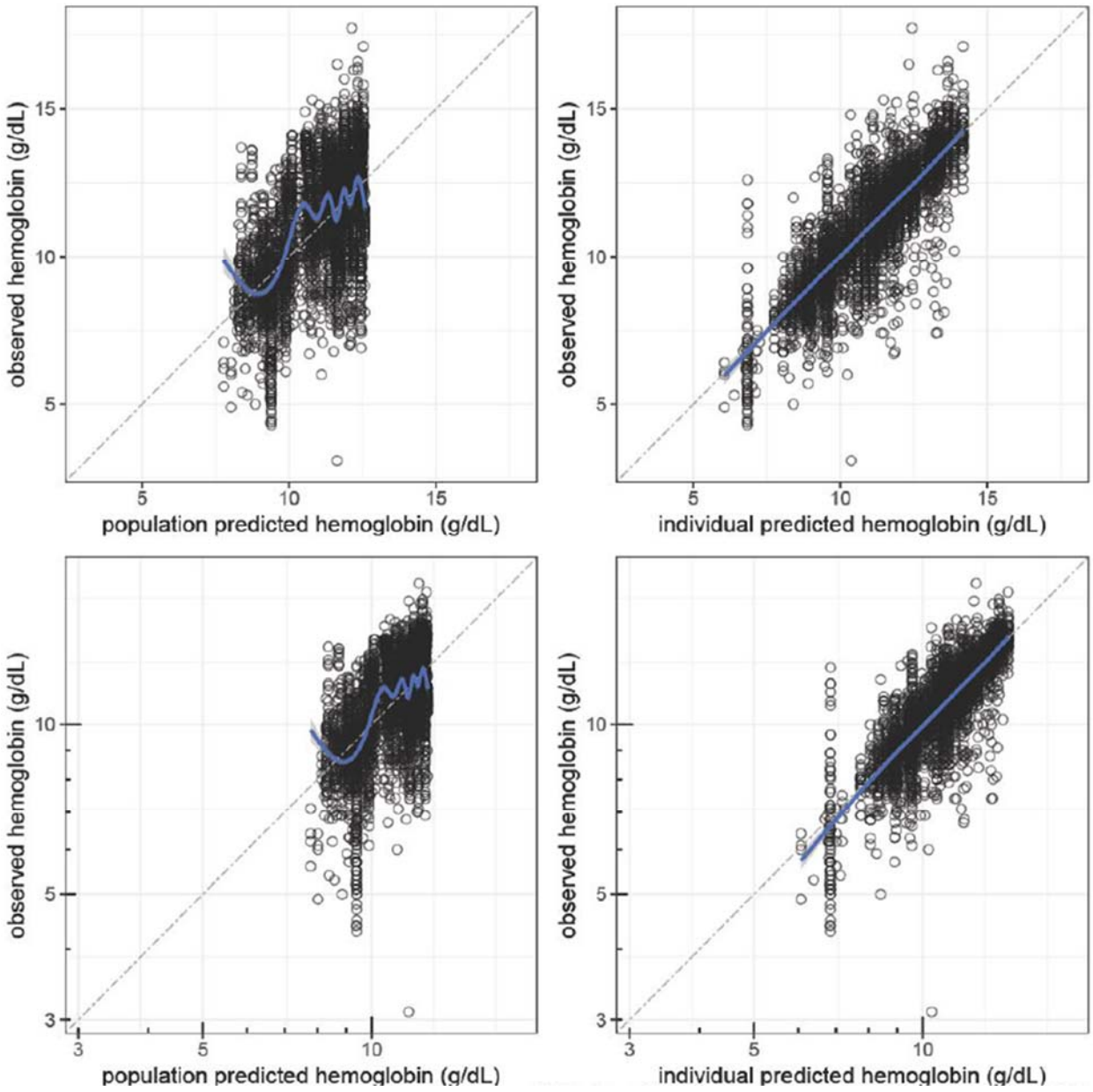

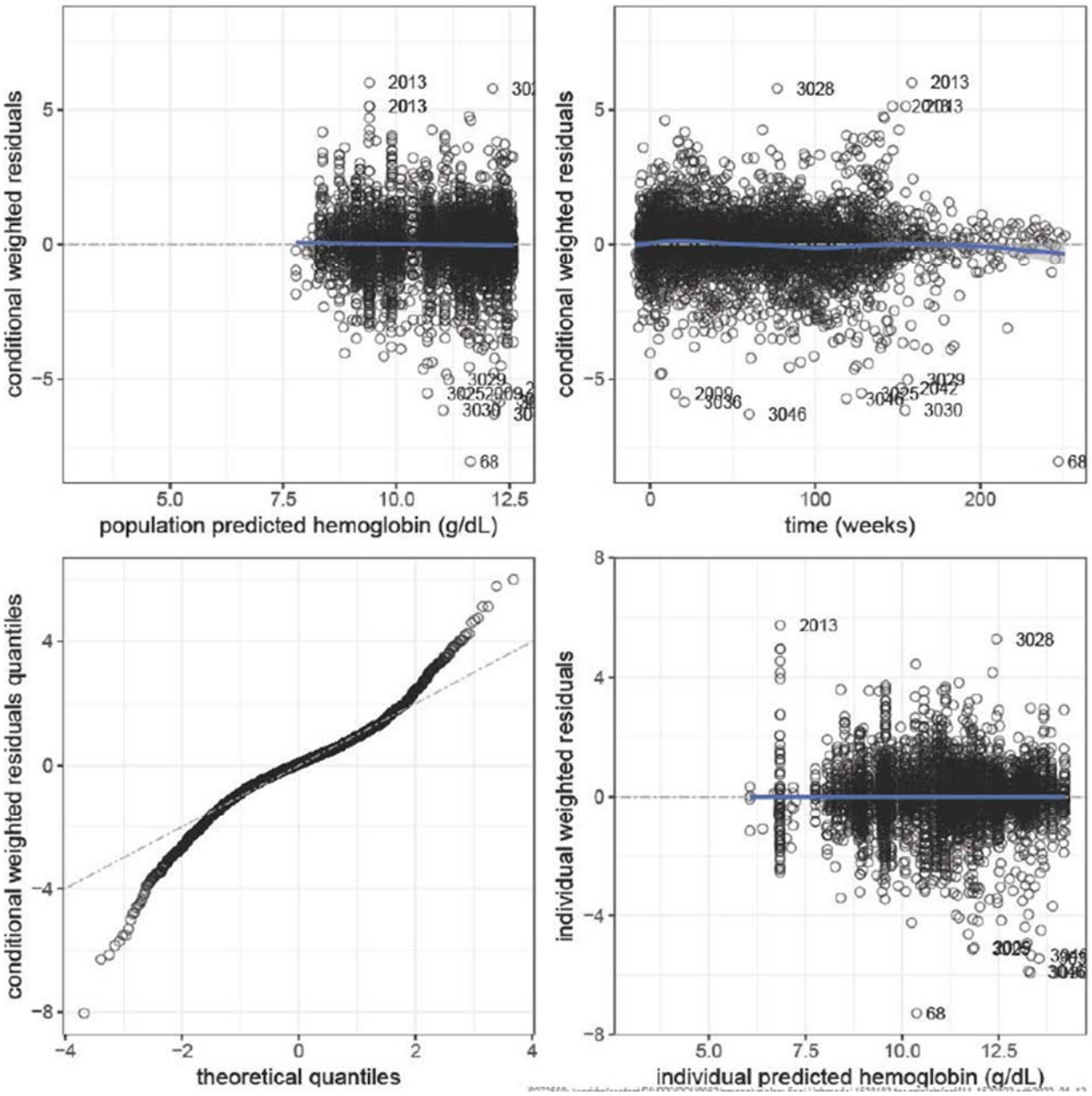

Supp. Fig. 7: The dashed line represents the identity line or zero line; the thick blue curve is the smoothing spline. Numbers indicate subject numbers with weighted residuals greater than 5 or less than -5.

PopPKPD, population pharmacokinetic/pharmacodynamic.

Supp. Fig. 8. Prediction-corrected VPC plot of Hb by time

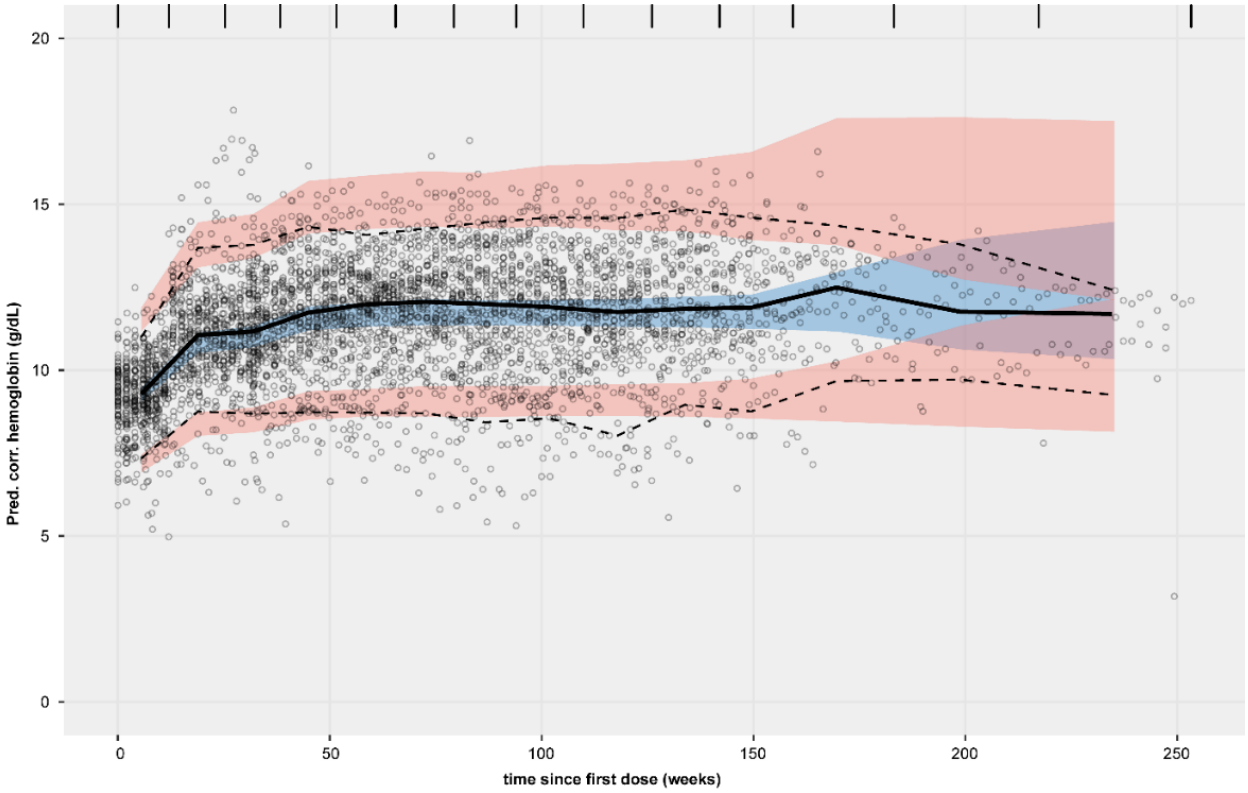

Hb, hemoglobin; VPC, visual predictive check.

Supp. Fig. 9. Prediction-corrected VPC plots for the PK/PD model stratified by dose (a), blood transfusion status (b), or renal function (c)

(a)

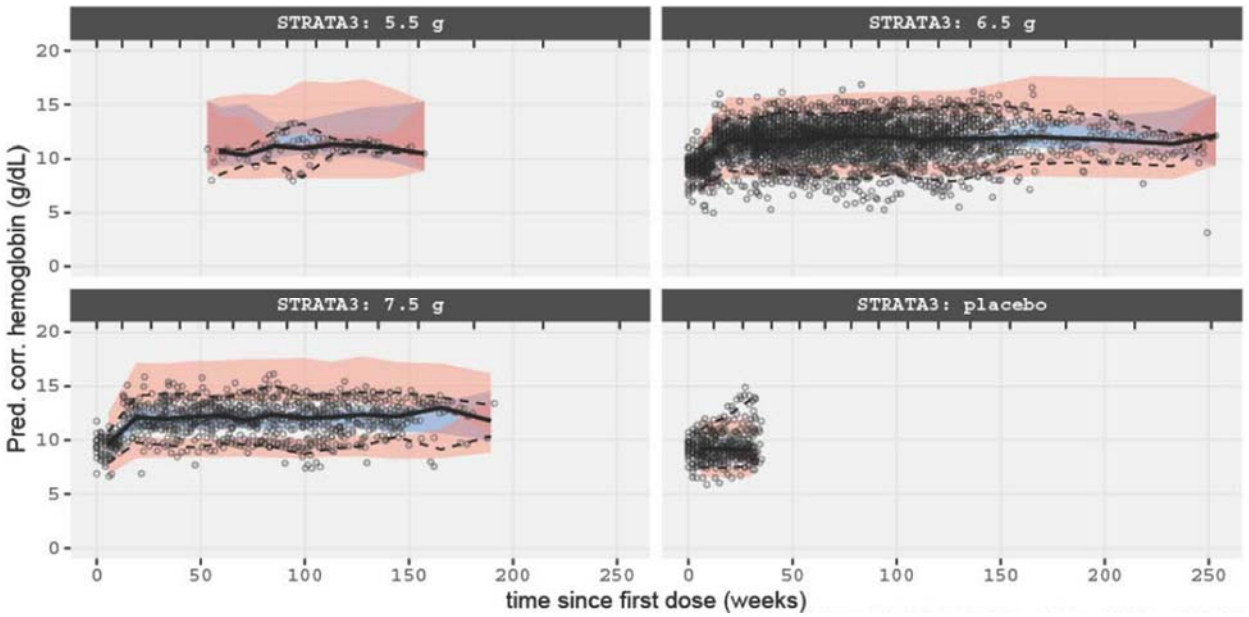

(b)

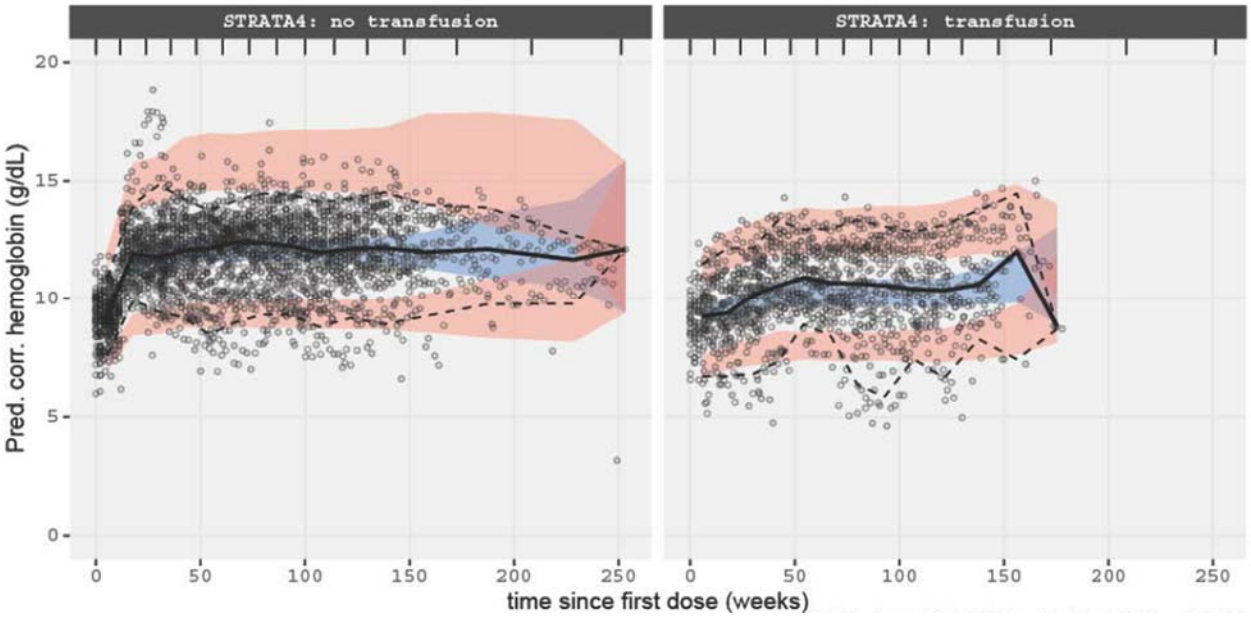

(c)

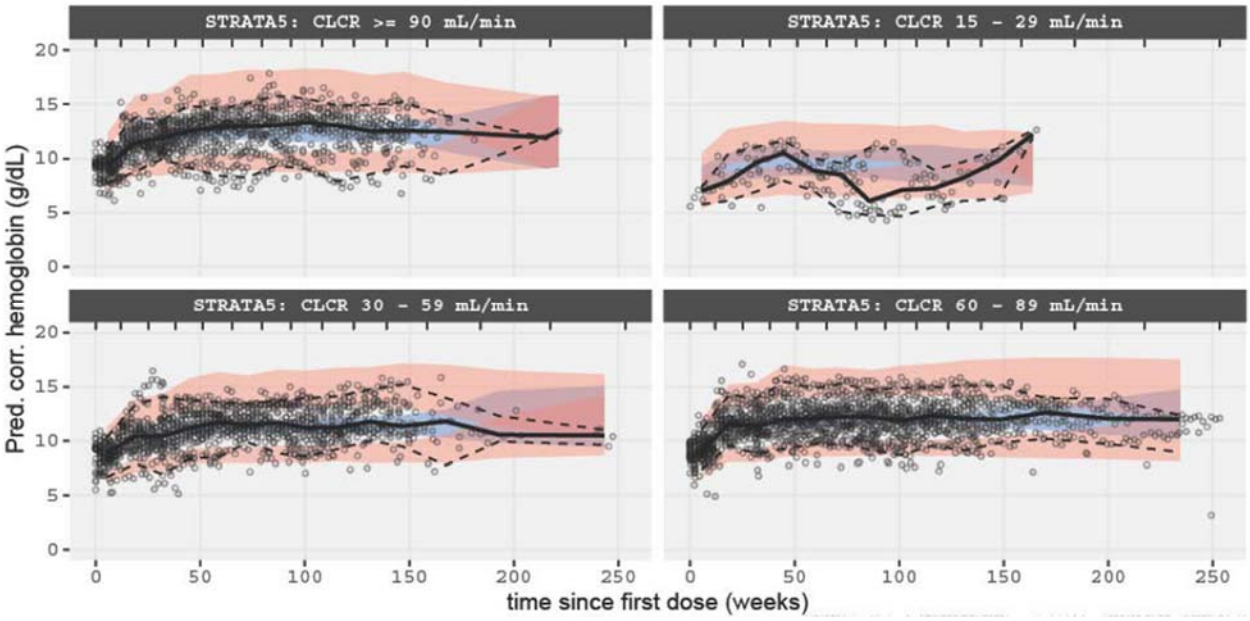

Supp. Fig. 9: Dots represent observations. The solid line represents the 50% percentile (median) of the observations. The observed 5% and 95% percentiles are presented with dashed lines. The shaded areas represent the 90% confidence interval around the 5%, 50% (median), and 95% percentiles of the simulations (n = 500 subproblem simulations).

PD, pharmacodynamic; PK, pharmacokinetic; VPC, visual predictive check.

Supp. Fig. 10. Normal Q-Q plot of NPDE, plot of NPDE vs. time and PRED, and histogram of NPDE with the probability density function of the overlaid standard Gaussian distribution.

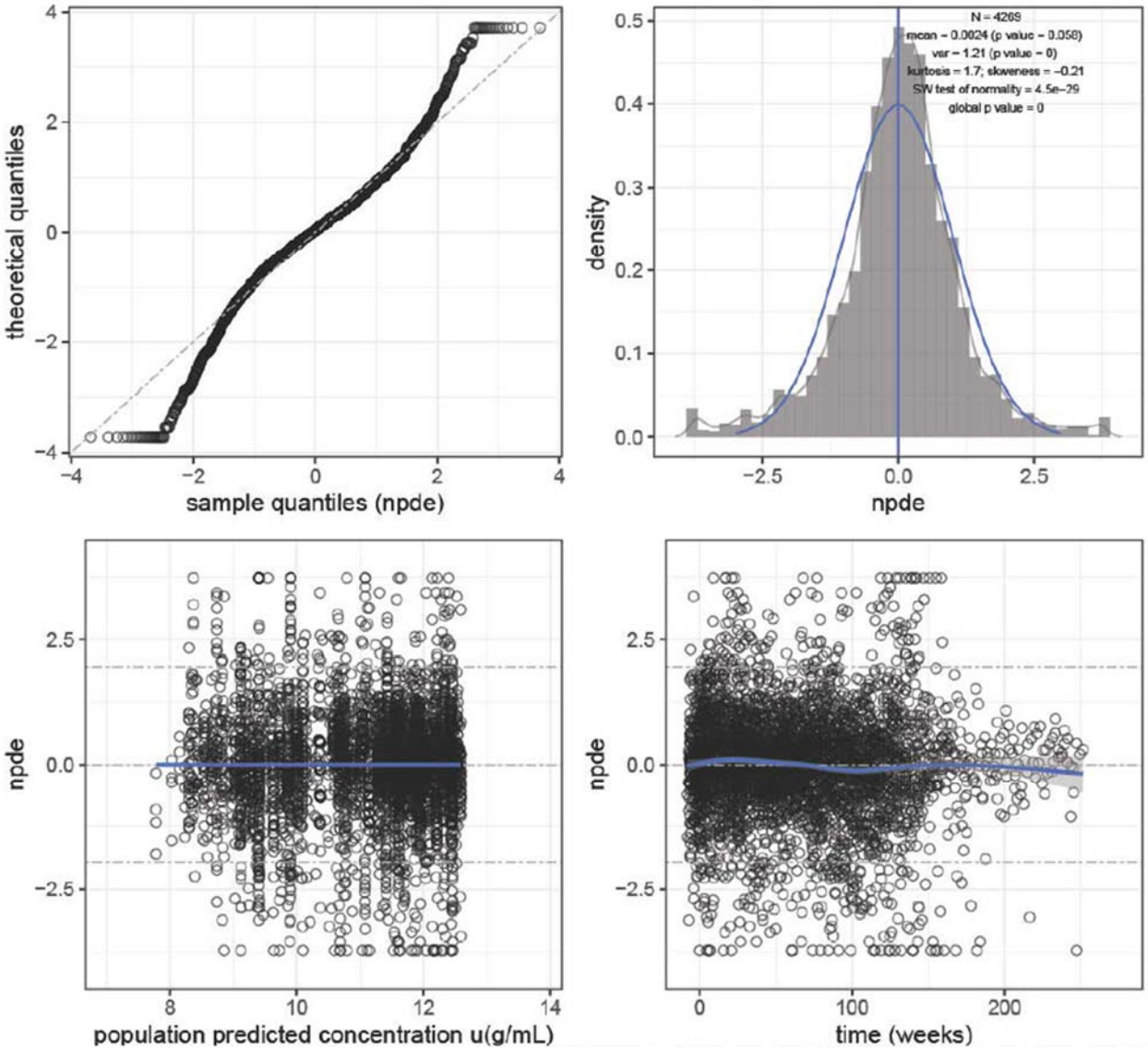

Supp. Fig. 10: The dashed line represents the identity line in Q-Q plot or the range between -1.96 and 1.96 in the plot of NPDE vs time and PRED; the thick blue curve is the smoothing spline.

NPDE, normalized prediction distribution errors; PRED, predicted data based on population parameter estimates; Q-Q, quantile-quantile.

Supp. Fig. 11. Relationship between hemoglobin change from baseline at steady state and (i) dose or (ii) $C_{min,ss}$ by weight (a), age (b), ethnicity (c), blood transfusion (d), and renal function (e)

(i)Dose

(a) Body weight (b) Age (c) Ethnicity

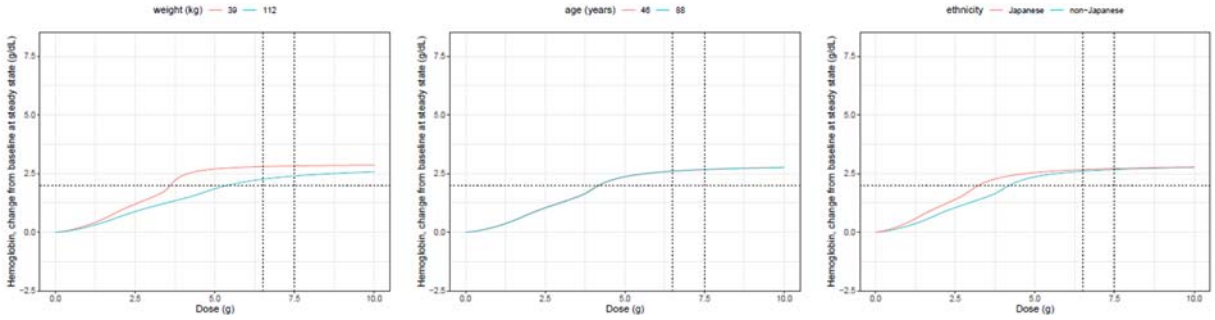

(d) Blood transfusion (e) Renal function

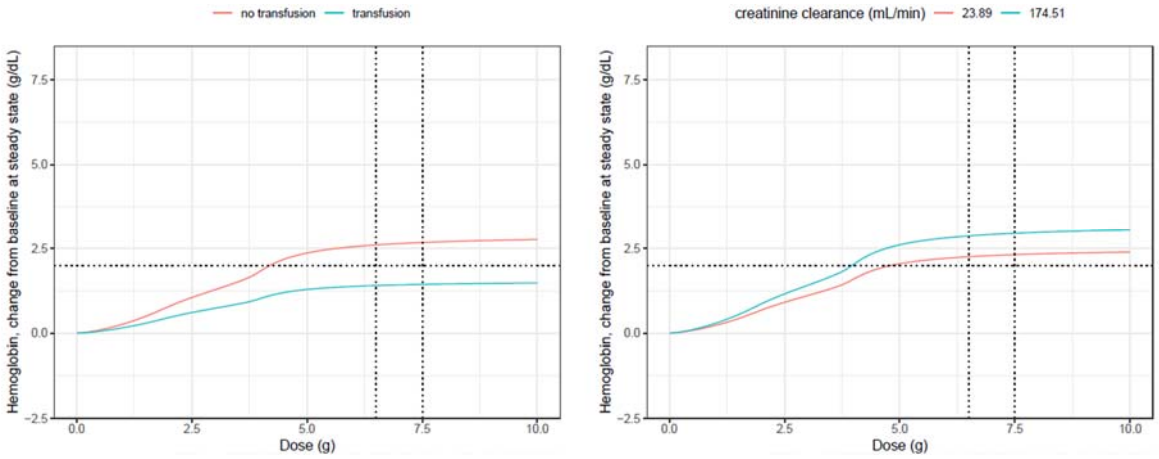

(ii) $C_{min,ss}$

(a) Body weight (b) Age (c) Ethnicity

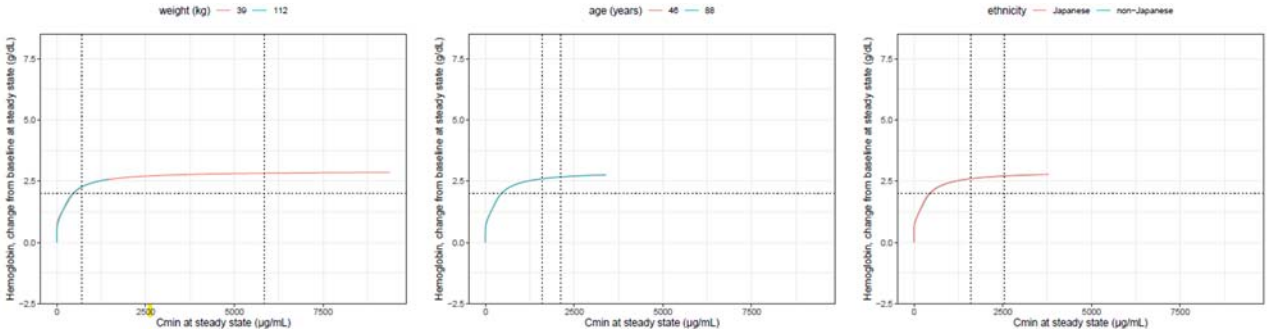

(d) Blood transfusion

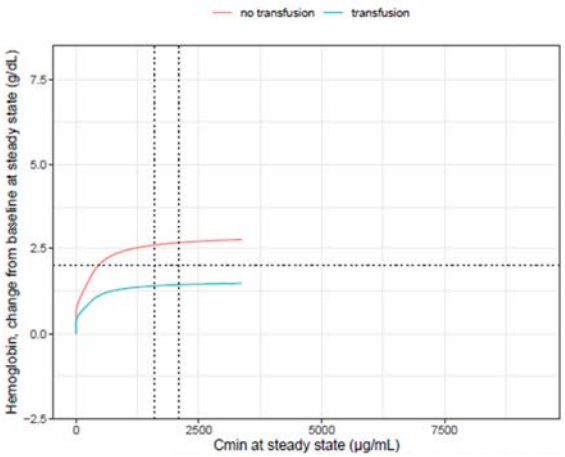

(e) Renal function

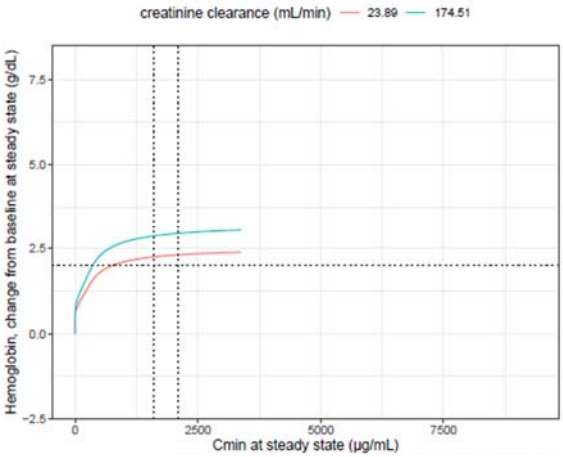

Supp. Fig. 11: The vertical dotted lines indicate the proposed therapeutic dosing. The horizontal line represents 2 g/dL hemoglobin change from baseline.

$C_{min,ss}$, minimum concentration.

Supp. Fig. 12. $AUC_{,ss}$ quartile plot of adverse events from BIVV009-03 and BIVV009-04 studies

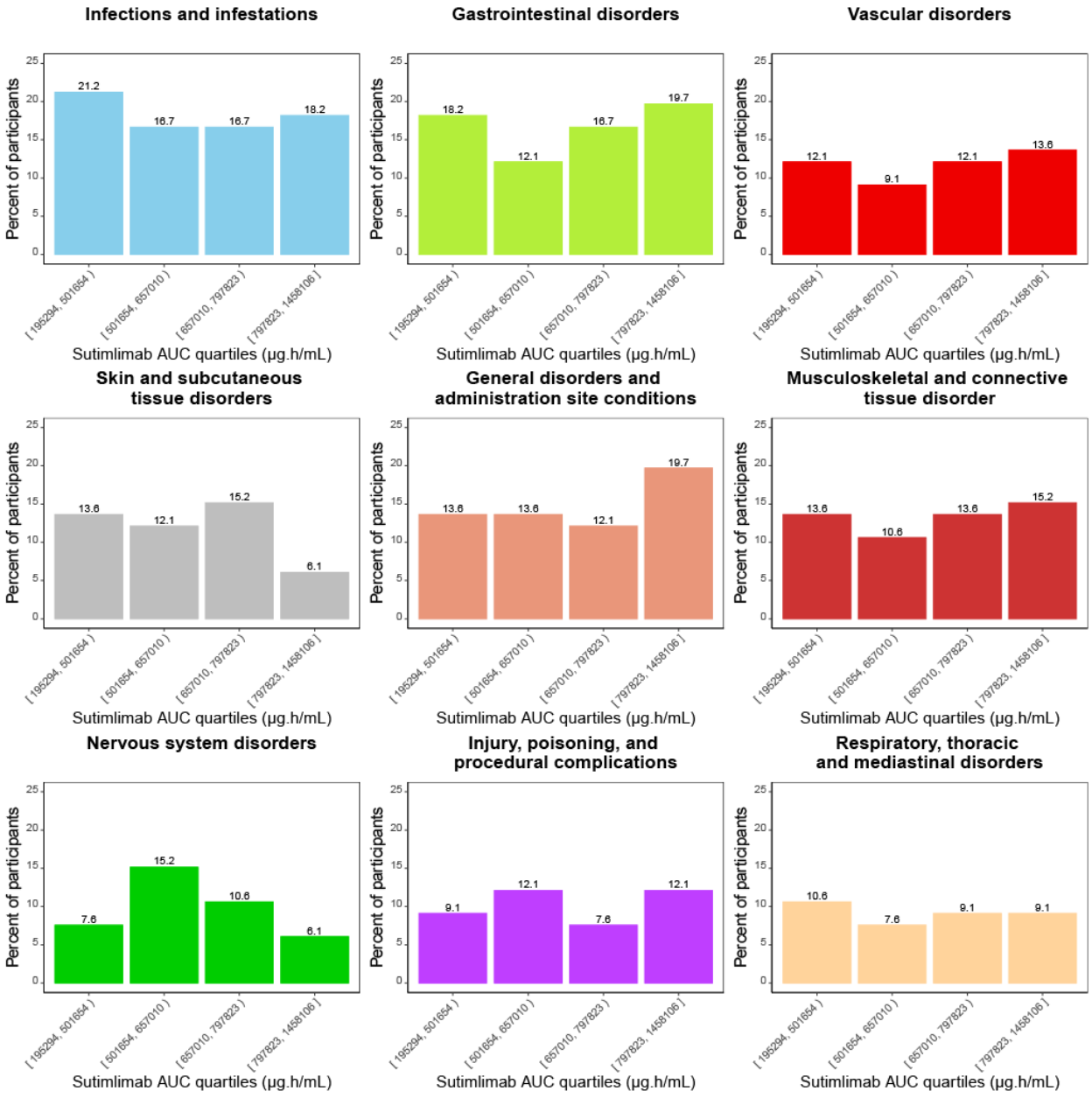

Supp. Fig. 12: Steady-state post hoc $AUC_{,ss}$ was estimated using population PK model for each participant. For each adverse event category, participants with positive event(s) were separated into four groups based on $AUC_{,ss}$ quartiles. The percentage of participants in each quartile group was calculated based on the total number of participants in BIVV009-03 and BIVV009-04 studies.

Supp. Fig. 13. $C_{max,ss}$ quartile plot of adverse events from BIVV009-03 and BIVV009-04 studies

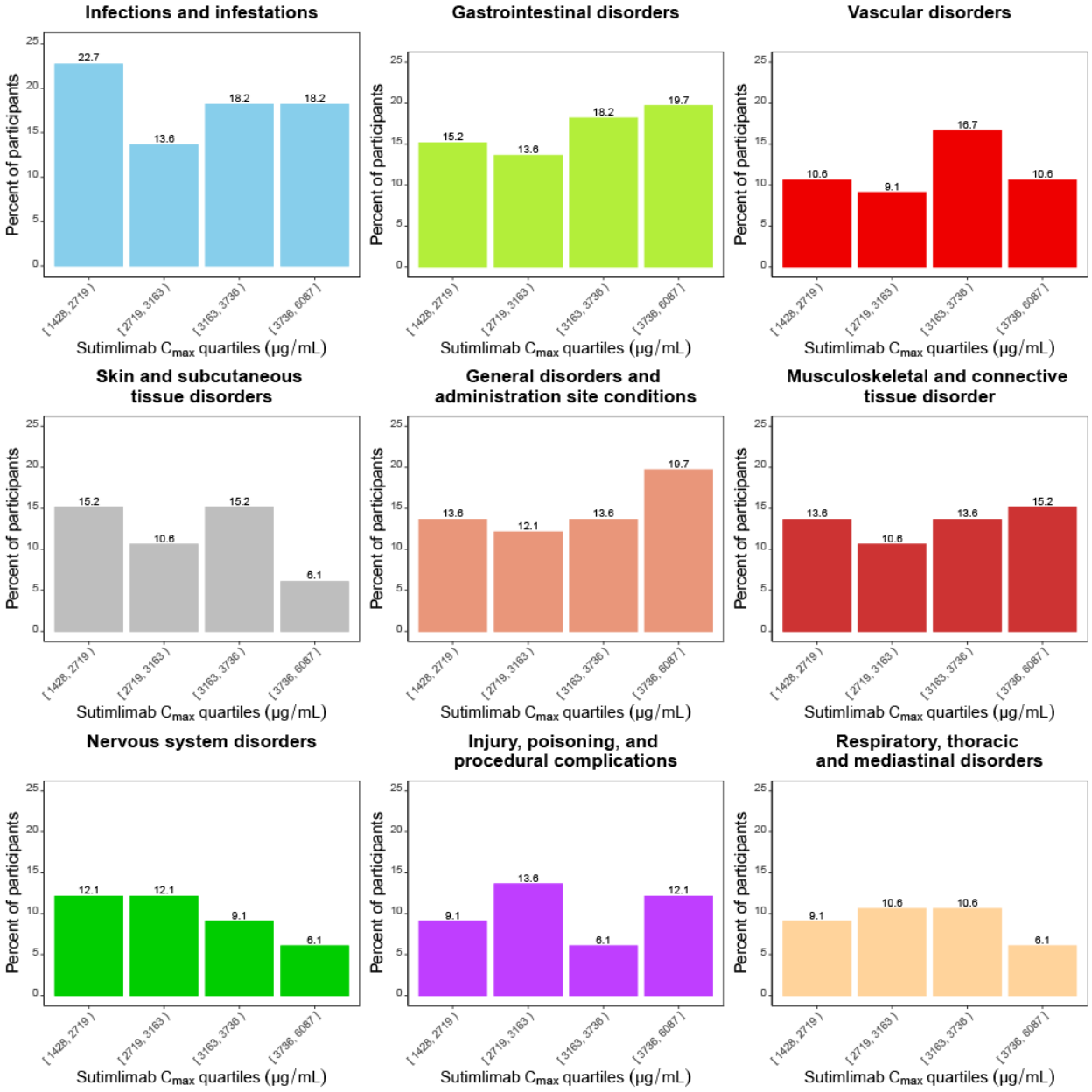

Supp. Fig. 13: Steady-state post hoc $C_{max,ss}$ was estimated using population PK model for each participant. For each adverse event category, participants with positive event(s) were separated into 4 groups based on $C_{max,ss}$ quartiles. The percentage of participants in each quartile group was calculated based on the total number of participants in BIVV009-03 and BIVV009-04 studies.

Supp. Fig. 14. Dose (in mg/kg) quartile plot of adverse events from BIVV009-03 and BIVV009-04 studies

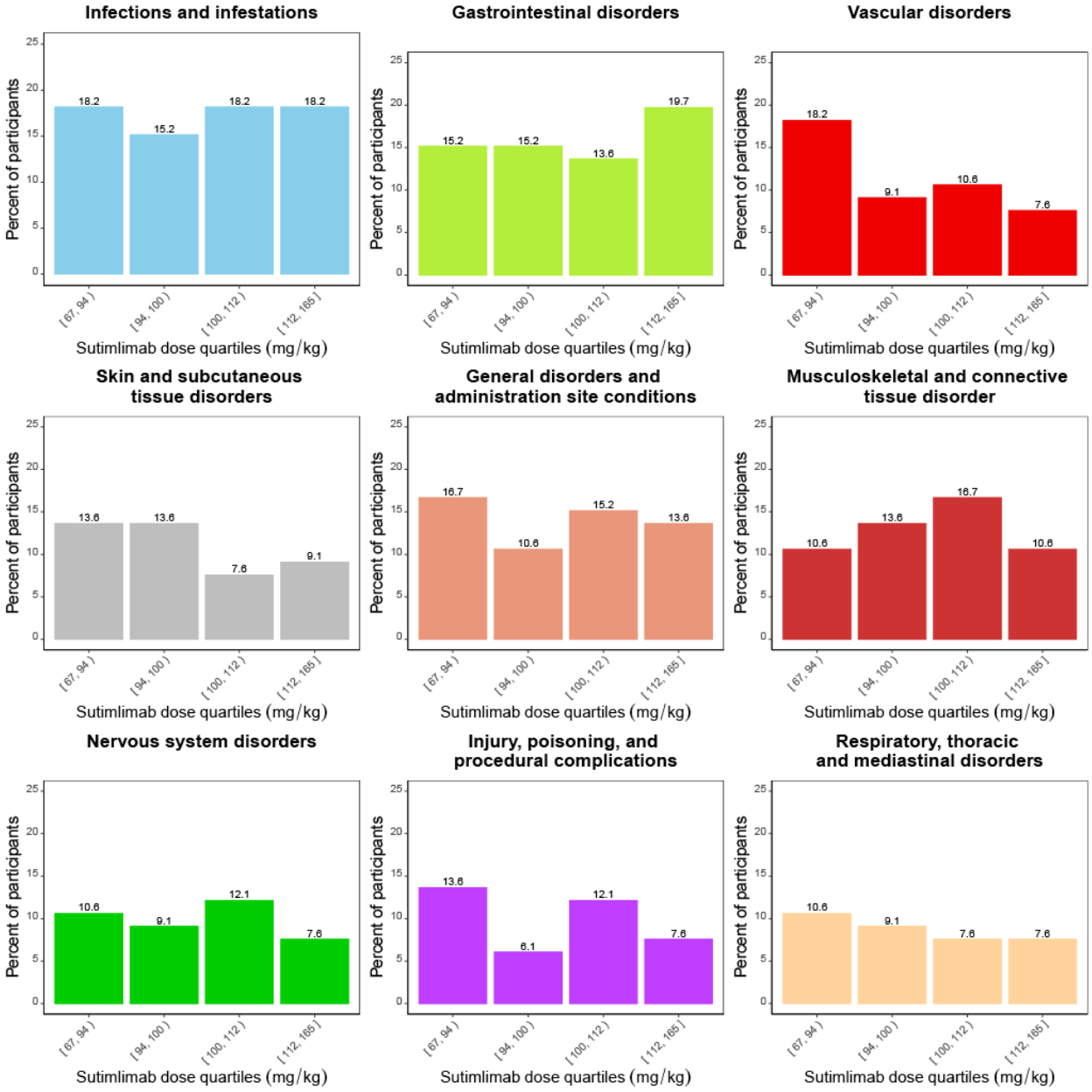

Supp. Fig. 14: For each adverse event category, participants with positive event(s) were separated into four groups based on dose (mg/kg) quartiles. The percentage of participants in each quartile group was calculated based on the total number of participants in BIVV009-03 and BIVV009-04 studies.

Supp. Fig. 15. Body weight quartile plot of adverse events from BIVV009-03 and BIVV009-04 studies

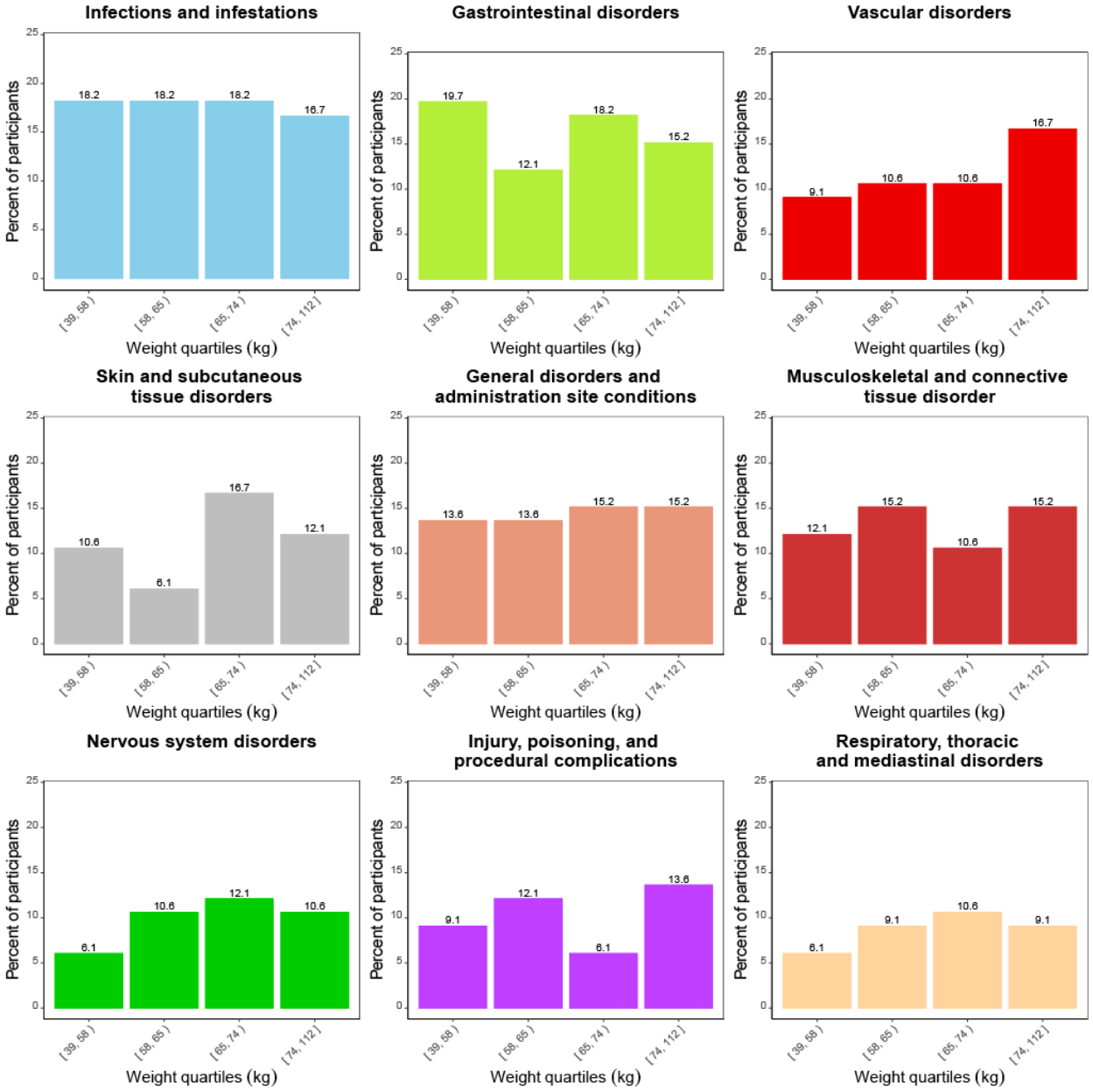

Supp. Fig. 15. For each adverse event category, participants with positive event(s) were separated into four groups based on body weight quartiles. The percentage of participants in each quartile group was calculated based on the total number of participants in BIVV009-03 and BIVV009-04.